

CRYSTALLOGRAPHIC EVALUATION OF CHELIDAMIC ACID CONGENERS

by

Austin L. Green

Submitted in partial fulfillment of the requirements for Departmental Honors in the  
Department of Chemistry at Texas Christian University in Fort Worth, Texas

May 4, 2015

CRYSTALLOGRAPHIC EVALUATION OF CHELIDAMIC ACID CONGENERS

Project Approved:

Kayla Green, Ph.D.

Department of Chemistry

(Supervising professor)

Julie Fry, Ph.D.

Department of Chemistry

Doug Ingram, Ph.D.

Department of Physics and Astronomy

**ABSTRACT**

Alzheimer's Disease, a progressive neurodegenerative disorder that takes the lives of approximately 500,000 people per year, still lacks a definitive diagnosis and reliable treatment protocol.<sup>1</sup> Oxidative stress has been shown to be a key factor associated with the molecular markers of the disease. As such, a series of N-heterocyclic amines derived from chelidamic acid have been produced to evaluate these compounds as potential therapeutics for Alzheimer's Disease targeting the molecular features associated with the progression of the disease. We have shown these systems to be both antioxidant and capable of breaking apart the plaques associated with this neurodegenerative disorder.<sup>2</sup> Based on the aforementioned success, this study focuses on the development of new systems based on a chelidamic acid core. My colleagues and I within the Green Research Group are interested in exploring the effects of electronic modifications to the chelidamic acid core on applications that includes the development of therapeutics for Alzheimer's Disease.

These chelidamic acid derivatives are characterized using X-ray crystallographic methods in order to show how the bond lengths and angles are influenced by the experimental R-groups, which possess a range of donor capacities. By comparing the structural results (bond angles and distances) from the range of proposed compounds, the influence of the varying donors on the aromatic ring can be understood. This information is critical for identifying optimal potential therapeutic agents prior to metallation.

**ACKNOWLEDGMENTS**

I acknowledge Dr. Kayla Green, my supervising professor, and the entirety of the Green Research Group. Without their endless work and dedication to producing novel chelidamic acid congeners, I could not have carried out my research project or written this thesis. Thanks to their efforts, I was able to solve their crystals and evaluate the resulting structures. I would like to thank TCU SERC for the financial support. Finally, I would like to thank my late sister, Molly Green, for inspiring me to pursue a career in the sciences.

**TABLE OF CONTENTS**

INTRODUCTION.....	1
Research Relevance.....	1
Materials and Methods.....	4
RESULTS AND DISCUSSION .....	8
Analysis of Compound 2.....	8
Analysis of Compound 4.....	9
Analysis of Compound 5.....	10
Structural Features of Compounds 2, 4, and 5.....	12
Analysis of Compound 3.....	19
CONCLUSIONS.....	23
SUPPORTING MATERIALS.....	24
REFERENCES .....	50

**LIST OF FIGURES**

1. The roles of metals in Alzheimer's Disease involves redox cycling to produce ROS that leads to cell death.....	1
2. Rational design of hybrid therapeutic models in the Green Research Group.....	3
3. Cu(II) and Zn(II) derivatives of <b>1-OH</b> .....	3
4. Drawings of structures pertinent to this project.....	6
5. Synthesis schematic for compounds <b>2</b> and <b>3</b> .....	6
6. Synthesis schematic for compounds <b>4</b> and <b>5</b> and (below) thermal ellipsoid plots (50%) of the solid-state structures.....	7
7. Labeling scheme for crystallographic data of <b>2</b> , <b>4</b> , and <b>5</b> .....	11
8. Unit cell for <b>2</b> showing the packing scheme.....	14
9. Unit cell for <b>4</b> showing the packing scheme.....	15
10. Unit cell for <b>5</b> showing the packing scheme.....	16
11. Thermal ellipsoid (50%) plot of <b>3</b> with labeling schemes adopted.....	18
12. Unit cell for <b>3</b> showing the packing scheme.....	19
13. Future synthesis pathway for the Green Research Group.....	23

**LIST OF TABLES**

1. Relevant bond lengths for <b>2</b> , <b>4</b> , and <b>5</b> .....	12
2. Experimental Details for <b>2-5</b> .....	17
3. Bond Lengths (Å) for <b>3</b> .....	21
4. Bond Angles (°) for <b>3</b> .....	22

## INTRODUCTION

### RESEARCH RELEVANCE

Alzheimer's Disease (AD) is a progressive neurodegenerative disorder that affects over five million individuals in the United States alone. With these numbers rapidly growing, the need for research with the eventual goal of proper diagnosis and treatment of AD is both great and urgent. This disease claims the lives of millions of individuals and is commonly characterized by increased oxidative stress and transition metal presence, as well as the deposition of  $\beta$ -amyloid ( $A\beta$ ) plaques. The crystallographic evaluation presented in this paper aims to assist in elucidating the effects of changing the electronic structure and thereby varying bond angles and lengths on the ability to decrease oxidative stress observed with derivatives of the compounds discussed herein.

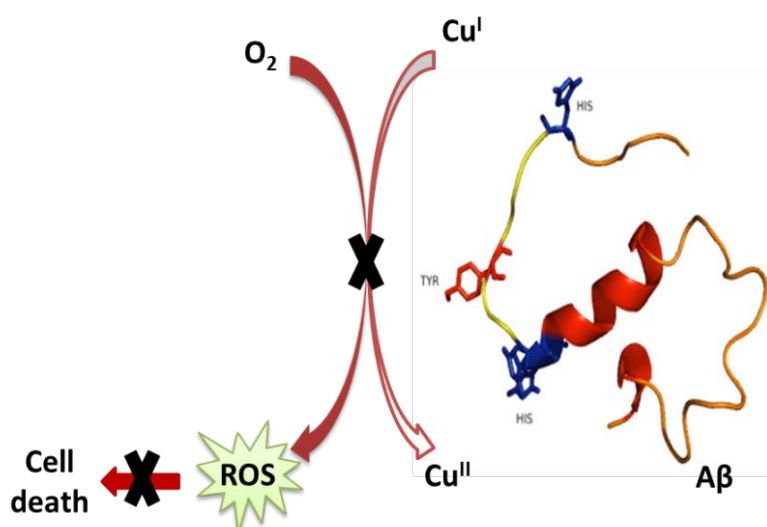


**Figure 1.** The roles of metals in Alzheimer's Disease involves redox cycling to produce ROS (reactive oxygen species) that leads to cell death.

In Alzheimer's Disease, redox-active metals aid in the aggregation of  $\beta$ -amyloid plaque in the brain, as shown in **Figure 1**. These redox-active metals engage in the reduction of  $O_2$  into reactive oxygen species (ROS), which leads to cell death, also demonstrated in **Figure 1**. Considering the role of metals in Alzheimer's Disease can easily be determined, the Green Research Group has been dedicated to finding solutions to combat these issues.

The Green Research Group has synthesized the structures shown in **Figure 3**. Using the example of **1-OH** from **Figure 2**, the cyclen-like portion of the molecule acts as a means of removing metals from amyloid and a means of stopping the redox reaction that allows for the formation of reactive oxygen species. In addition, the hydroxyl group acts as a radical scavenger, effectively quenching the reactive oxygen species that are created. Previous research in the Green Research Group has show this compound to be highly antioxidant and a strong binding agent for metals, as shown in **Figure 2**. This multimodal approach at treatment leads to a potentially effective therapeutic agent for Alzheimer's Disease.

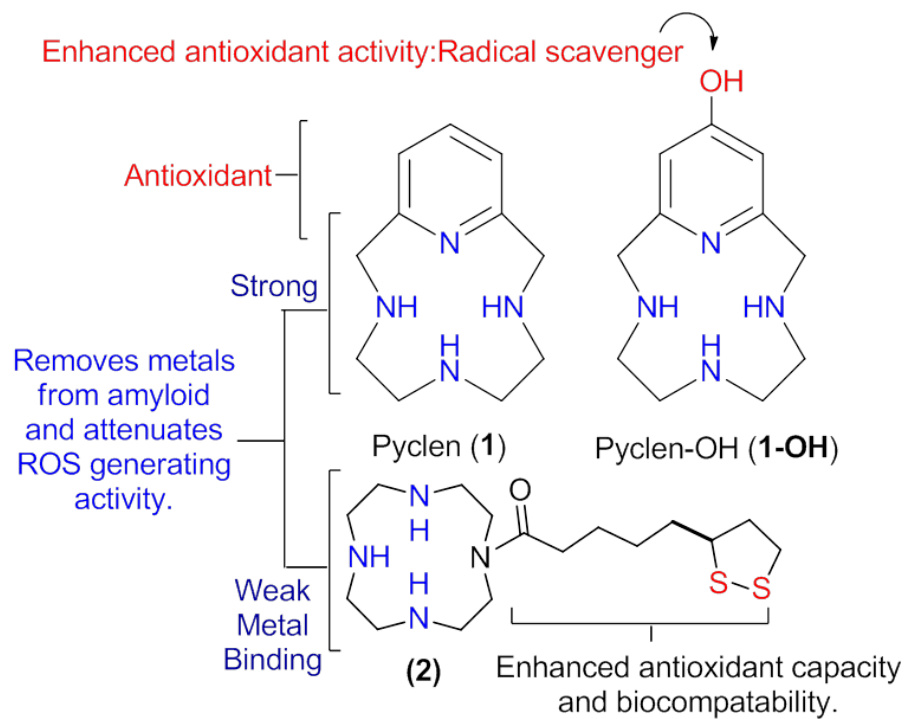


**Figure 2.** Rational design of hybrid therapeutic models in the Green Research Group.

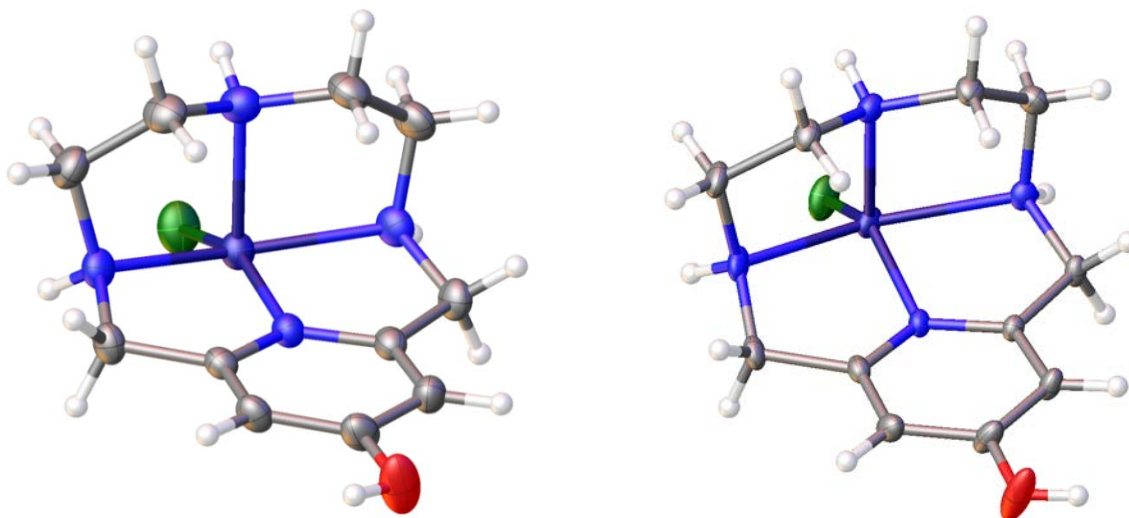


**Figure 3.** Cu(II) and Zn(II) derivatives of 1-OH.

## MATERIALS AND METHODS

X-ray crystallographic methods were employed to produce the data presented in this paper. The XRD instrument used to obtain this data is available free of charge in conjunction with the Department of Chemistry at TCU. All purchases of chemicals and items needed to run the XRD instrument were made through commercial sources and include the liquid nitrogen necessary for low-temperature data collection and the CryoLoops needed to mount the crystals.

The crystals obtained for evaluation were produced from commercially available reagents and were synthesized by co-workers Brittney Chaney and Zack Dekam. These co-workers focused on the purification of the compounds derived from chelidamic acid (4-Hydroxypyridine-2,6-dicarboxylic Acid Monohydrate, shown in **Figure 4**). These derivatives were produced using modified methods from the literature. Upon obtaining crystals suitable for X-ray analysis, the crystals were then separated to find a sample suitable for evaluation through X-ray diffraction methods.

A Leica MZ 75 microscope was used to identify samples suitable for analysis. A Bruker Apex 2 X-ray (three-circle) diffractometric was employed for crystal screening and unit cell determination. The data collections were obtained at 100 K. The goniometer was controlled using the APEX2 software suite, v2008-6.0. The samples were optically centered with the aid of a video camera such that no translations were observed as the crystal was rotated through all positions. The X-ray radiation employed was generated from a Mo sealed X-ray tube ( $K_{\alpha} = 0.70173\text{\AA}$  with a potential of 40 kV and a current of 40 mA) fitted with a graphite

monochromator in the parallel mode (175 mm collimator with 0.5 mm pinholes). The crystal-to-detector distance was set to 50 mm and the exposure time was 10 s per degree for all data sets at a scan width of 0.5°. The frames were integrated with the Bruker SAINT Software package using a narrow-frame algorithm. Data were corrected for absorption effects using the multi-scan method (SADABS). Structural refinements were performed with Xshell (v 6.3.1) by the full-matrix least-squares method. All hydrogen and non-hydrogen atoms were refined using anisotropic thermal parameters. The ORTEP molecular plots (50 %) were produced using Olex2.

The basis of this research stems from a chelidamic acid core, which has been used in various projects in the Green Research Group to synthesize compounds that are both antioxidant and capable of breaking down beta-amyloid plaques associated with AD.<sup>2</sup> I have structurally characterized the congener compounds of chelidamic acid shown in **Figure 1**. It is important to structurally characterize these systems using X-ray crystallographic methods in order to show how the bond lengths and angles are influenced by the functionalization of the pyridol core, which possess a range of donor capacities. X-ray crystallography is equivalent to providing a picture of the compounds of interest, and therefore provides electronic characterization of the compound when used in combination with general bonding concepts derived from general and organic chemistry coursework. By comparing the structural results (bond angles and distances) from the range of compounds, the influence of the varying donors on the aromatic ring will be evident. This information will be tied into concurrent studies in the Green Research Group looking at these

compounds as catalysts for C-C bond formation and continued work as therapeutic agents for Alzheimer's Disease.

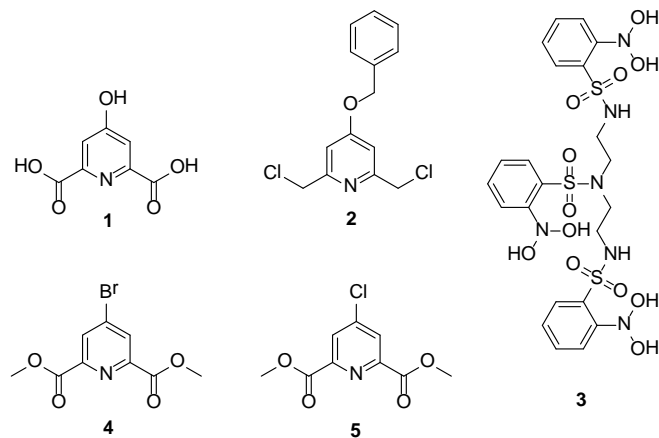


**Figure 4.** Drawings of structures pertinent to this project.

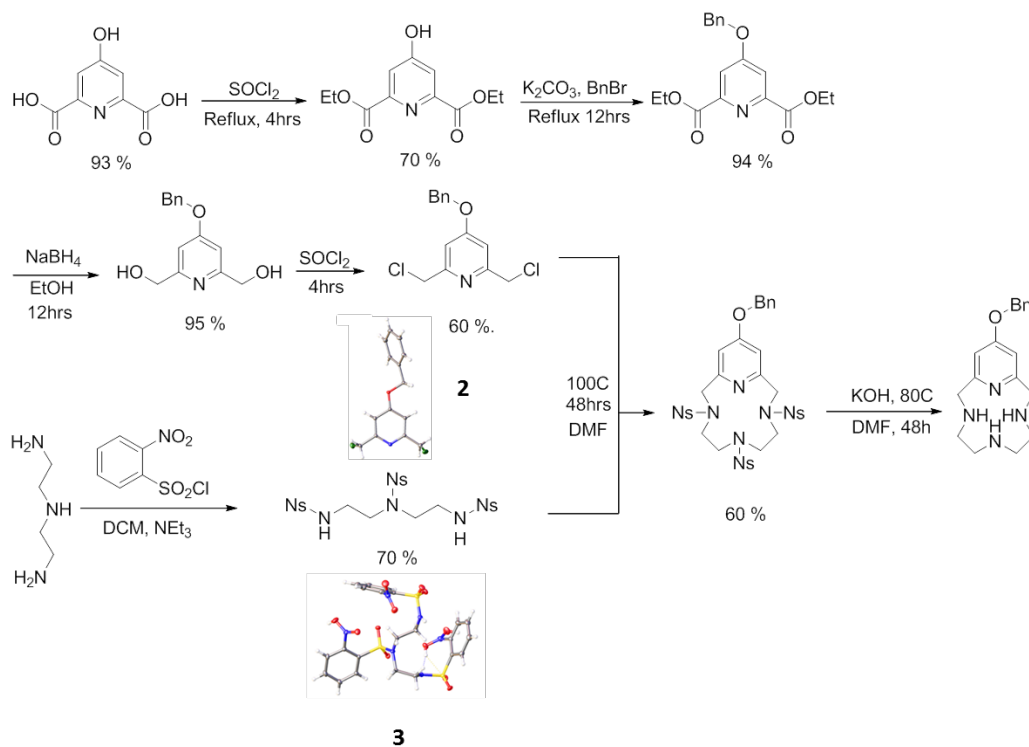


**Figure 5.** Synthesis schematic for compounds **2** and **3**.

The Green Research Group has adopted several methodologies in an attempt to synthesize inexpensive novel potential therapeutic agents for Alzheimer's Disease. Through this goal, the synthetic pathway revealed in **Figure 5** has been utilized as a means of synthesizing the desired compounds. In order to learn more about the intermediate compounds throughout this pathway, crystals of several intermediates were grown in the laboratory setting and these crystals were analyzed using X-ray crystallographic methods in order to determine pertinent information about compounds **2** and **3**, shown in **Figure 5**. Notably structure **3** is a prevalent compound used throughout the research conducted in the Green Research Group. The details obtained through X-ray crystallographic methods are the first attempts at determining the bond lengths and angles for this particular structure.

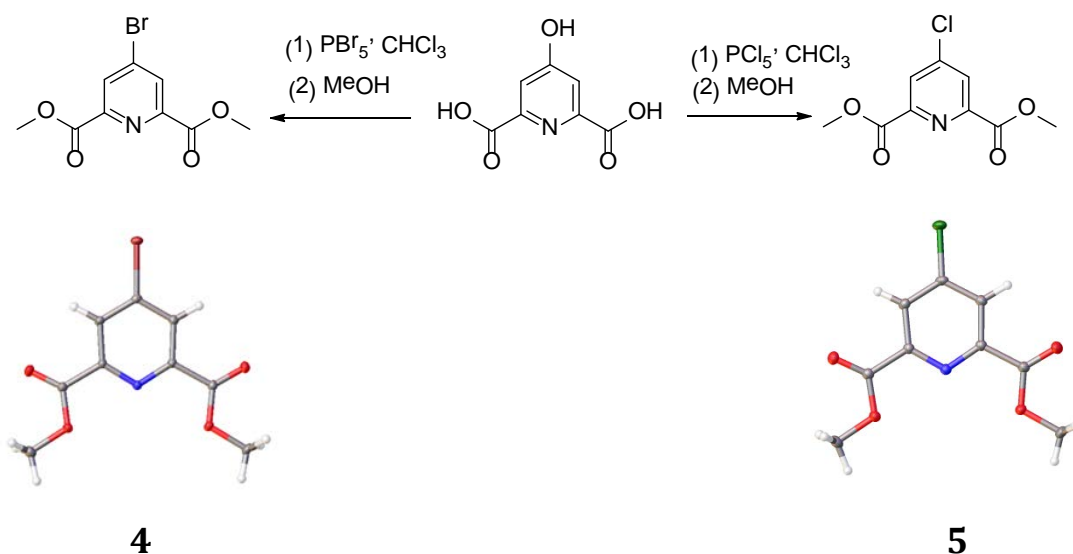


**Figure 6.** Synthesis schematic for compounds **4** and **5** and (below) thermal ellipsoid plots (50%) of the solid-state structures.

The Green Research Group has worked with various divergent synthetic pathways in attempt to study the effects of the functionalization of the pyridol core. **Figure 6** details one of said divergent synthetic pathways, both obtained in high yields by co-workers Zackery Dekam (**4**) and Brittney Chaney (**5**) using methodology established in the literature.<sup>3</sup> The research of this synthetic pathway clarifies the differences in bond lengths and angles on corresponding bonds between the structures in order to see how the electronics of the structure change throughout the synthetic process.

## RESULTS AND DISCUSSION

### Analysis of Compound 2.

For compound **2**, shown in **Figure 7**, a lustrous light brown cube-like specimen of  $C_{14}H_{13}Cl_2NO$ , approximate dimensions 0.147 mm x 0.579 mm x 0.678 mm, was used for the X-ray crystallographic analysis. The X-ray intensity data were measured.

A total of 1472 frames were collected. The total exposure time was 4.09 hours. The frames were integrated with the Bruker SAINT software package using a narrow-frame algorithm. The integration of the data using a monoclinic unit cell yielded a total of 30281 reflections to a maximum  $\theta$  angle of  $35.16^\circ$  (0.62 Å resolution), of which 5408 were independent (average redundancy 5.599, completeness = 95.3%,  $R_{int} = 2.15\%$ ,  $R_{sig} = 1.19\%$ ) and 5114 (94.56%) were greater than  $2\sigma(F^2)$ . The final cell parameters of  $a = 13.8984(16)$  Å,  $b = 7.9572(9)$  Å,  $c = 12.2990(14)$  Å,  $\beta = 110.485(2)^\circ$ , volume =  $1274.2(3)$  Å<sup>3</sup>, are based upon the

refinement of the XYZ-centroids of 9963 reflections above  $20 \sigma(I)$  with  $6.222^\circ < 2\theta < 70.19^\circ$ . Data were corrected for absorption effects using the multi-scan method (SADABS). The ratio of minimum to maximum apparent transmission was 0.909. The calculated minimum and maximum transmission coefficients (based on crystal size) are 0.7300 and 0.9310.

The final anisotropic full-matrix least-squares refinement on  $F^2$  with 163 variables converged at  $R1 = 2.82\%$ , for the observed data and  $wR2 = 8.18\%$  for all data. The goodness-of-fit was 0.996. The largest peak in the final difference electron density synthesis was  $0.523 \text{ e}^-/\text{\AA}^3$  and the largest hole was  $-0.511 \text{ e}^-/\text{\AA}^3$  with an RMS deviation of  $0.069 \text{ e}^-/\text{\AA}^3$ . On the basis of the final model, the calculated density was  $1.471 \text{ g/cm}^3$  and  $F(000)$ , 584 e<sup>-</sup>.

#### **Analysis of Compound 4.**

For compound **4**, as shown in **Figure 7**, a clear, colourless plate-like specimen of  $\text{C}_{18}\text{H}_{16}\text{Br}_2\text{N}_2\text{O}_8$ , approximate dimensions  $0.055 \text{ mm} \times 0.289 \text{ mm} \times 0.660 \text{ mm}$ , was used for the X-ray crystallographic analysis. The X-ray intensity data were measured.

A total of 2948 frames were collected. The total exposure time was 8.19 hours. The frames were integrated with the Bruker SAINT software package using a narrow-frame algorithm. The integration of the data using a triclinic unit cell yielded a total of 50238 reflections to a maximum  $\theta$  angle of  $36.60^\circ$  ( $0.60 \text{ \AA}$  resolution), of which 9622 were independent (average redundancy 5.221, completeness = 98.6%,  $R_{\text{int}} = 4.01\%$ ,  $R_{\text{sig}} = 3.01\%$ ) and 8149 (84.69%) were greater than  $2\sigma(F^2)$ . The final cell parameters of  $\underline{a} = 3.9490(4) \text{ \AA}$ ,  $\underline{b} = 13.6106(15) \text{ \AA}$ ,  $\underline{c} = 18.741(2) \text{ \AA}$ ,  $\alpha =$

$98.424(3)^\circ$ ,  $\beta = 92.952(3)^\circ$ ,  $\gamma = 97.707(3)^\circ$ , volume =  $984.82(18) \text{ \AA}^3$ , are based upon the refinement of the XYZ-centroids of 9706 reflections above  $20 \sigma(I)$  with  $6.115^\circ < 2\theta < 72.93^\circ$ . Data were corrected for absorption effects using the multi-scan method (SADABS). The ratio of minimum to maximum apparent transmission was 0.595. The calculated minimum and maximum transmission coefficients (based on crystal size) are 0.1700 and 0.8030.

The final anisotropic full-matrix least-squares refinement on  $F^2$  with 275 variables converged at  $R1 = 3.22\%$ , for the observed data and  $wR2 = 7.40\%$  for all data. The goodness-of-fit was 1.082. The largest peak in the final difference electron density synthesis was  $0.819 \text{ e}/\text{\AA}^3$  and the largest hole was  $-0.501 \text{ e}/\text{\AA}^3$  with an RMS deviation of  $0.114 \text{ e}/\text{\AA}^3$ . On the basis of the final model, the calculated density was  $1.848 \text{ g}/\text{cm}^3$  and  $F(000)$ , 544 e<sup>-</sup>.

### **Analysis of Compound 5.**

In regards to compound **5**, as shown in **Figure 7**, a clear, colourless specimen of  $\text{C}_9\text{H}_8\text{ClNO}_4$ , approximate dimensions  $0.006 \text{ mm} \times 0.170 \text{ mm} \times 0.681 \text{ mm}$ , was used for the X-ray crystallographic analysis. The X-ray intensity data were measured.

A total of 1472 frames were collected. The total exposure time was 4.09 hours. The frames were integrated with the Bruker SAINT software package using a narrow-frame algorithm. The integration of the data using a monoclinic unit cell yielded a total of 19228 reflections to a maximum  $\theta$  angle of  $30.60^\circ$  ( $0.70 \text{ \AA}$  resolution), of which 2919 were independent (average redundancy 6.587, completeness = 98.3%,  $R_{\text{int}} = 3.98\%$ ,  $R_{\text{sig}} = 2.57\%$ ) and 2386 (81.74%) were

greater than  $2\sigma(F_2)$ . The final cell parameters of  $a = 3.8202(12) \text{ \AA}$ ,  $b = 13.770(4) \text{ \AA}$ ,  $c = 18.224(6) \text{ \AA}$ ,  $\beta = 91.070(8)^\circ$ , volume =  $958.5(5) \text{ \AA}^3$ , are based upon the refinement of the XYZ-centroids of 9523 reflections above  $20 \sigma(I)$  with  $6.326^\circ < 2\theta < 61.20^\circ$ .

Data were corrected for absorption effects using the multi-scan method (SADABS).

The ratio of minimum to maximum apparent transmission was 0.867. The calculated minimum and maximum transmission coefficients (based on crystal size) are 0.7770 and 0.9980.

The final anisotropic full-matrix least-squares refinement on  $F_2$  with 169 variables converged at  $R_1 = 3.27\%$ , for the observed data and  $wR_2 = 8.91\%$  for all data. The goodness-of-fit was 1.056. The largest peak in the final difference electron density synthesis was  $0.476 \text{ e-/\AA}^3$  and the largest hole was  $-0.234 \text{ e-/\AA}^3$  with an RMS deviation of  $0.066 \text{ e-/\AA}^3$ . On the basis of the final model, the calculated density was  $1.591 \text{ g/cm}^3$  and  $F(000)$ , 472 e-.

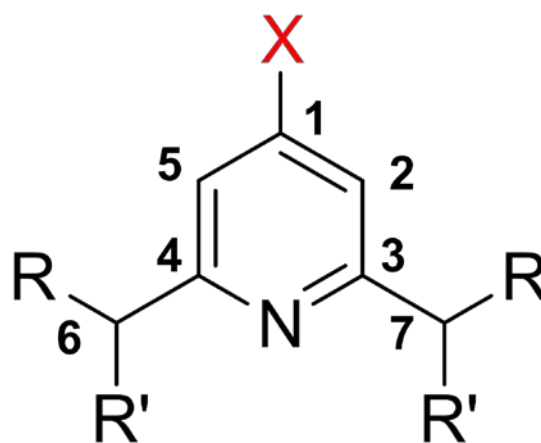


**Figure 7.** Labeling scheme for crystallographic data of 2, 4, and 5.

**Table 1.** Relevant bond lengths for **2**, **4**, and **5**.

Bond	2	4	5
<b>C1-X</b>	[X=OBz] 1.3561(7)	[X=Br] 1.8818(13)	[X=Cl] 1.7369(5)
<b>C1-C2</b>	1.3968(9)	1.3882(19)	1.3860(3)
<b>C2-C3</b>	1.3903(9)	1.3952(19)	1.3987(4)
<b>C3-N</b>	1.3421(8)	1.3348(18)	1.3387(3)
<b>N-C4</b>	1.3411(8)	1.3395(17)	1.3393(3)
<b>C4-C5</b>	1.3954(9)	1.3956(19)	1.4011(4)
<b>C5-C1</b>	1.3977(9)	1.385(2)	1.3881(3)
<b>C3-C7</b>	1.5005(9)	1.5069(18)	1.5071(4)
<b>C4-C6</b>	1.4994(9)	1.4993(19)	1.5096(4)

**Structural Features of Compounds 2, 4, and 5.**

The relevant bond lengths for compounds **2**, **4**, and **5**, as seen in **Table 1**, are the bonds in the aromatic ring and the first bond off of the aromatic ring in any direction. The corresponding bond angles for all three of these compounds were found to be equivalent, with only negligible differences between each other, which was expected due to the stringency of aromatic systems. In addition, the bond lengths on the aromatic ring and extending out of the ring onto the adjacent carbons in the meta-position from the X-groups, shown in **Figure 7** and **Table 1**, are all approximately equivalent for the corresponding bonds in each compound. This is also expected due to these bond lengths being in an aromatic system and also because there are no other electronic effects acting upon the involved carbons that differ in any of those compounds.

The notable difference between compounds **2**, **4**, and **5** is in the C1-X bond. These bonds noticeably differ in each compound. As expected, the C1-Cl bond in **5** is shorter than the C1-Br bond in **4**, seen in **Table 1**, as a result of the greater electronegativity of Cl pulling electron density away from the carbon atom, thus decreasing the bond length. Compound **2**, notably, has a C1-OBz bond length that is significantly shorter than the C1-Cl bond of compound **5**. This means that the OBz group is able to attract significantly more electron density from the carbon atom closer to the group than the Cl atom can. This results from the high electronegativity of an oxygen atom, augmented by the benzyl group acting as an electron withdrawing group on that oxygen atom, thus further shortening the bond.

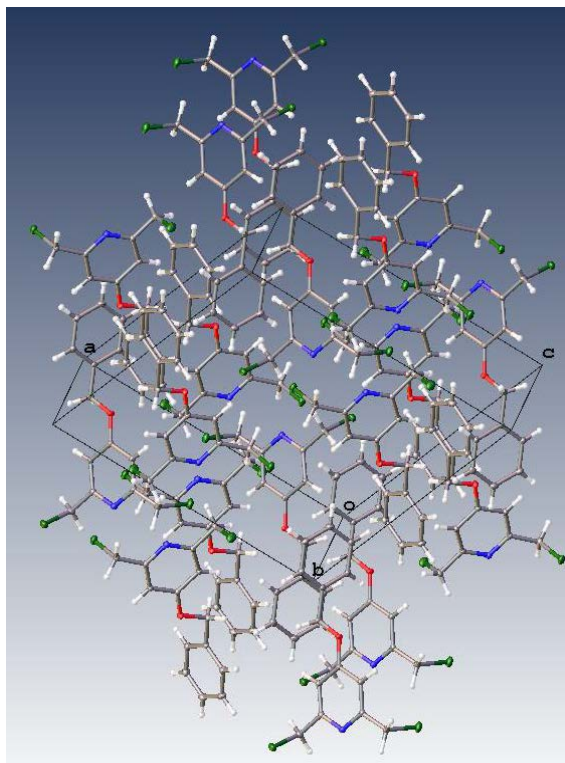


**Figure 8.** Unit cell for **2** showing the packing scheme.

The packing diagram for compound **2** is shown in **Figure 8**. The unit cell contains four molecules of **2**, which are held together by dipole-dipole forces. Due to the twisting of the  $sp^3$  carbon,  $\pi$ -stacking is inhibited. These conclusions are based on the aromatic components of the unit cell being roughly  $7.9 \text{ \AA}$  apart from each other, meaning that  $\pi$ -stacking is not a component of the packing scheme. Therefore, dipole-dipole forces are the strongest force acting upon these molecules and thus create the pattern for crystallization.

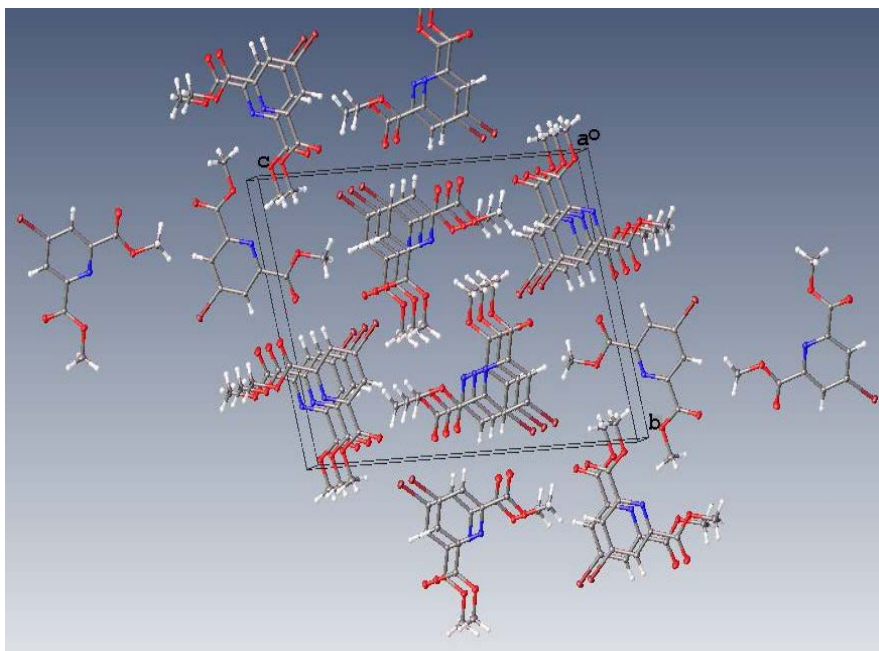


**Figure 9.** Unit cell for **4** showing the packing scheme.

The packing diagram for compound **4** is shown in **Figure 9**. There are two molecules of the compound in the unit cell. For this compound, the method of lattice formation is  $\pi$ -stacking, where the pi bonds overlap each other.  $\pi$ -stacking is commonly operationally defined as having a difference of less than 4.9 Å between molecules. In the case of compound **4**, there is a difference of 3.949 Å. Thus, the driving force behind the crystallization of **4** can be attributed to  $\pi$ -stacking.

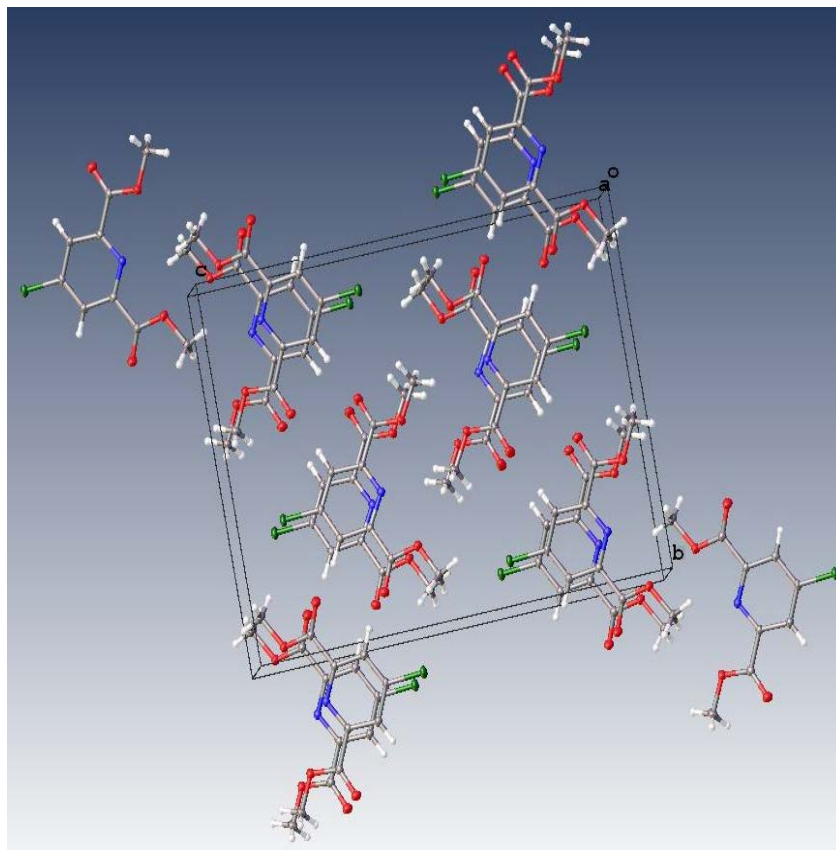


**Figure 10.** Unit cell for **5** showing the packing scheme.

The packing diagram for compound **5** is shown in **Figure 10**. There are four molecules of compound **5** per unit cell. Much like compound **4**, there is no solvent present in the unit cell, meaning that the solvent is irrelevant for its crystal lattice formation. The underlying mechanism behind the crystallization of **5** is  $\pi$ -stacking, as the molecules are 3.820 Å apart, which is 1.18 Å beneath the requisite 4.9 Å difference for  $\pi$ -stacking. This distance is shorter than the distance between molecules in compound **4**, since Cl is a smaller atom than Br, meaning that the molecules can be closer together.

**Table 2.** Experimental details for **2-5**.

<b>Complex</b>	<b>2</b>	<b>3</b>	<b>4</b>	<b>5</b>
<b>Chemical Formula</b>	C <sub>14</sub> H <sub>13</sub> Cl <sub>2</sub> NO	C <sub>28</sub> H <sub>22</sub> O <sub>12</sub> S <sub>3</sub> N <sub>4</sub>	C <sub>18</sub> H <sub>16</sub> Br <sub>2</sub> N <sub>2</sub> O <sub>8</sub>	C <sub>9</sub> H <sub>8</sub> NO <sub>4</sub> Cl
<b>Formula Weight (g/mol)</b>	282.15	661.68	548.15	229.62
<b>Crystal System</b>	Monoclinic	Monoclinic	Triclinic	Monoclinic
<b>Space Group</b>	P 1 21/c 1	P 21/c	P -1	P21/n
<b>a (Å)</b>	13.8984(16)	17.180(17)	3.9490(4)	3.8202(12)
<b>b (Å)</b>	7.9572(9)	12.454(11)	13.6106(15)	13.770(4)
<b>c (Å)</b>	12.2990(14)	12.337(13)	18.741(2)	18.224(6)
<b>α (°)</b>	90	90	98.424(3)	90
<b>β (°)</b>	110.485(2)	92.57(3)	92.952(3)	91.070(8)
<b>γ (°)</b>	90	90	97.707(3)	90
<b>Volume (Å<sup>3</sup>)</b>	1274.2(3)	2637(4)	984.82(18)	958.5(5)
<b>Z</b>	4	4	2	4
<b>Density (g/cm<sup>3</sup>)</b>	1.471	1.666	1.848	1.5911
<b>Reflections Collected</b>	30281	171912	50238	19228
<b>Independent Reflections</b>	5408 [R <sub>int</sub> = 0.0215]	14843 [R <sub>int</sub> = 0.0482, R <sub>sigma</sub> = 0.0409]	9622 [R <sub>int</sub> = 0.0401]	2919 [R <sub>int</sub> = 0.0398, R <sub>sigma</sub> = 0.0257]
<b>Goodness-of-fit on F<sup>2</sup></b>	0.996	1.093	1.082	1.116
<b>R1 I&gt;2σ(I)</b>	0.0282	0.0489	0.0322	0.0328
<b>wR2 I&gt;2σ(I)</b>	0.0799	0.1399	0.0693	0.0863
<b>R1</b>	0.03	0.0851	0.0437	0.0438
<b>wR2</b>	0.0818	0.1627	0.0740	0.0983

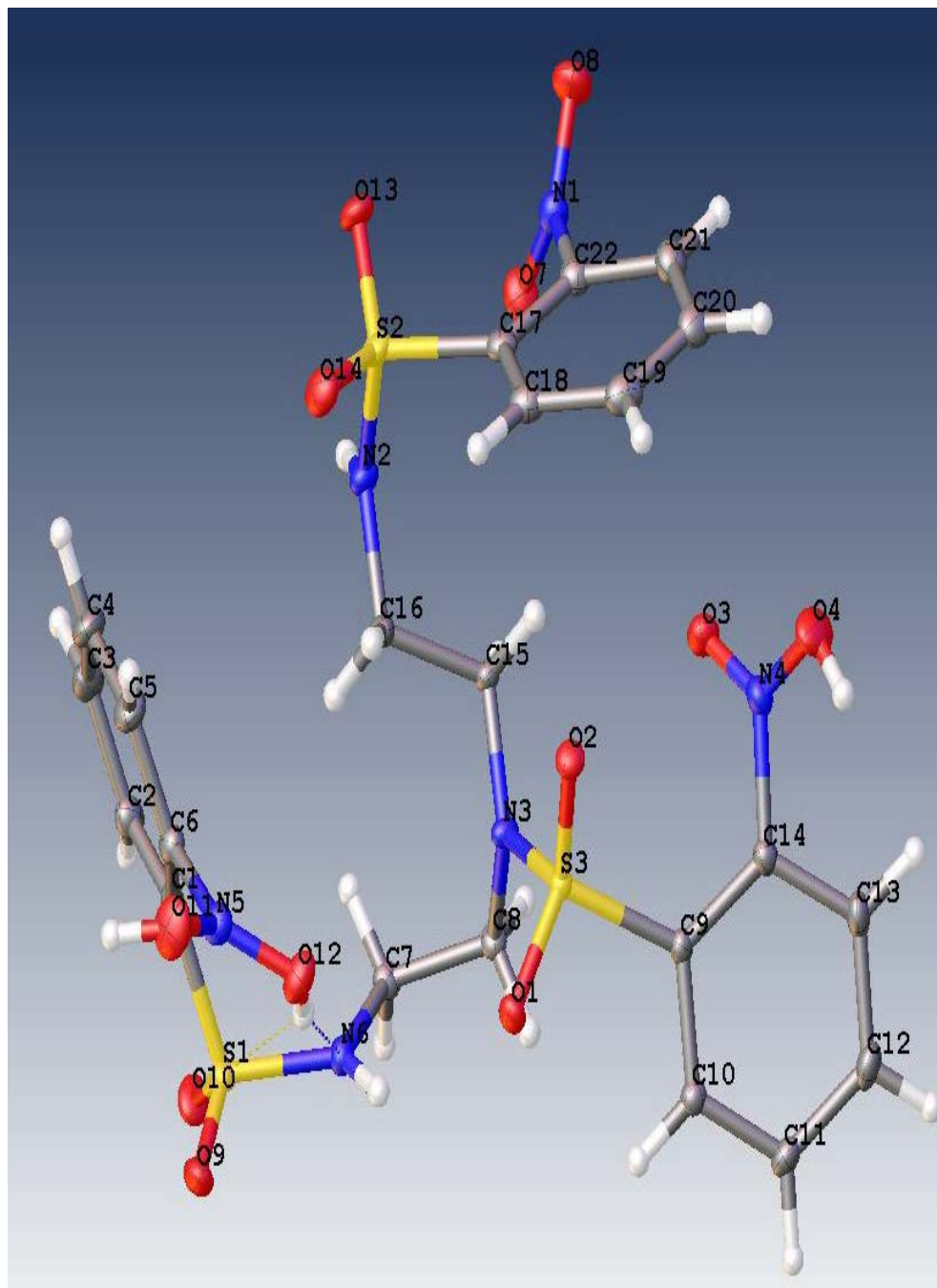


**Figure 11.** Thermal ellipsoid (50%) plot of **3** with labeling schemes adopted.

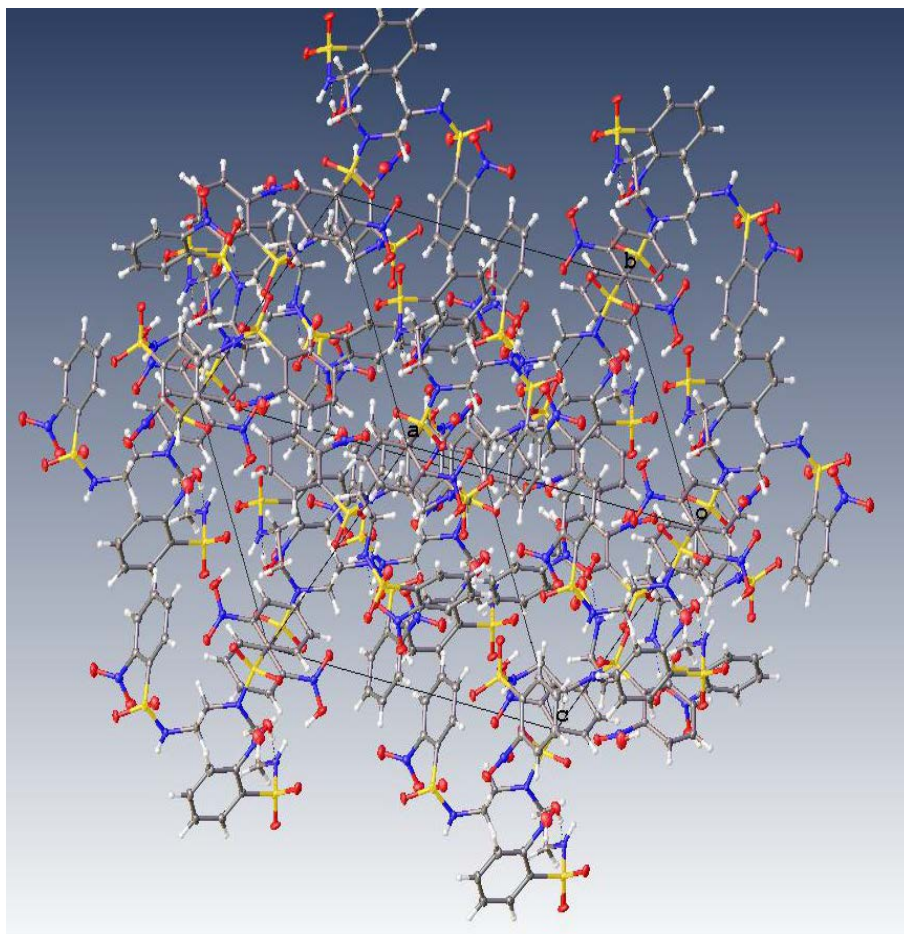


**Figure 12.** Unit cell for **3** showing the packing scheme.

### **Analysis of Compound 3.**

For compound **3**, as seen in **Figure 11** and **Figure 12**, a specimen of  $C_{28}H_{22}N_4O_{12}S_3$ , approximate dimensions 0.130 mm x 0.210 mm x 0.440 mm, was used for the X-ray crystallographic analysis. The X-ray intensity data were measured.

The integration of the data using a monoclinic unit cell yielded a total of 171912 reflections to a maximum  $\theta$  angle of  $38.61^\circ$  (0.57 Å resolution), of which 14843 were independent (average redundancy 11.582, completeness = 99.3%, Rint

= 4.82%,  $R_{sig} = 4.09\%$ ) and 10476 (70.58%) were greater than  $2\sigma(F_2)$ . The final cell parameters of  $a = 17.180(17) \text{ \AA}$ ,  $b = 12.454(11) \text{ \AA}$ ,  $c = 12.337(13) \text{ \AA}$ ,  $\beta = 92.57(3)^\circ$ , volume =  $2637.4(4) \text{ \AA}^3$ , are based upon the refinement of the XYZ-centroids of reflections above  $20 \sigma(I)$ . The calculated minimum and maximum transmission coefficients (based on crystal size) are 0.8577 and 0.9545.

The structure was solved and refined using the Bruker SHELXTL Software Package, using the space group  $P 1 21/c 1$ , with  $Z = 4$  for the formula unit,  $C_{28}H_{22}N_4O_{12}S_3$ . The final anisotropic full-matrix least-squares refinement on  $F_2$  with 391 variables converged at  $R_1 = 4.90\%$ , for the observed data and  $wR_2 = 15.90\%$  for all data. The goodness-of-fit was 1.068. The largest peak in the final difference electron density synthesis was  $0.815 \text{ e-/\AA}^3$  and the largest hole was  $-0.906 \text{ e-/\AA}^3$  with an RMS deviation of  $0.122 \text{ e-/\AA}^3$ . On the basis of the final model, the calculated density was  $1.770 \text{ g/cm}^3$  and  $F(000)$ , 1448 e-.

The triply Ns-protected derivative of diethylene triamine is a staple in the heterocyclic literature. However, and to the best of our knowledge, this is the first X-ray crystallographic characterization of this compound to date. The crystals of the characterization of the compound were obtained by slow evaporation in organic solvents. This structure acts in a way that folds upward and facilitates the cyclization required for the formation of heterocyclic compounds, which the Green Research Group uses as a means of metal capture to help prevent the redox reaction responsible for the creation of reactive oxygen species in the brain.

**Table 3.** Bond Lengths (Å) for **3**.

S1	O9	1.4275(15)	C18	C19	1.394(2)
S1	O10	1.4261(15)	C19	C20	1.382(2)
S1	C1	1.775(2)	C20	C21	1.386(2)
S1	N6	1.6131(16)	C9	C14	1.3979(19)
S2	O13	1.4302(15)	C9	C10	1.391(2)
S2	N2	1.6147(17)	C14	C13	1.3827(19)
S2	C17	1.7715(18)	C14	N4	1.468(2)
S2	O14	1.4236(14)	C13	C12	1.390(2)
S3	O1	1.4351(12)	C12	C11	1.389(2)
S3	O2	1.4289(15)	C11	C10	1.3885(19)
S3	N3	1.6114(18)	C21	C22	1.377(2)
S3	C9	1.7817(16)	C22	N1	1.467(2)
O3	N4	1.2207(17)	C2	C3	1.396(2)
O4	N4	1.2193(16)			
O7	N1	1.2293(17)			
O8	N1	1.2190(17)			
O11	N5	1.2230(16)			
O12	N5	1.2220(16)			
C4	C5	1.385(2)			
C4	C3	1.376(2)			
C5	C6	1.379(2)			
C6	C1	1.398(2)			
C6	N5	1.463(2)			
C1	C2	1.385(2)			
N6	C7	1.4651(19)			
C7	C8	1.520(2)			
C8	N3	1.4707(18)			
N3	C15	1.4677(18)			
C15	C16	1.5279(19)			
C16	N2	1.4625(19)			
C17	C18	1.387(2)			
C17	C22	1.398(2)			

**Table 4.** Bond Angles (°) for **3**.

O10	S1	O9	119.40(6)	N2	C16	C15	110.64(10)
C1	S1	O9	108.14(6)	C16	N2	S2	119.81(9)
C1	S1	O10	106.13(6)	C18	C17	S2	118.95(10)
N6	S1	O9	108.48(6)	C22	C17	S2	123.00(9)
N6	S1	O10	106.41(6)	C22	C17	C18	117.87(12)
N6	S1	C1	107.78(5)	C19	C18	C17	120.18(12)
N2	S2	O13	106.78(6)	C20	C19	C18	120.36(12)
C17	S2	O13	107.21(6)	C21	C20	C19	120.50(13)
C17	S2	N2	108.12(6)	C14	C9	S3	125.10(9)
O14	S2	O13	120.77(6)	C10	C9	S3	116.64(8)
O14	S2	N2	107.41(6)	C10	C9	C14	118.05(10)
O14	S2	C17	106.04(6)	C13	C14	C9	121.97(11)
O2	S3	O1	119.36(5)	N4	C14	C9	122.08(10)
N3	S3	O1	107.01(5)	N4	C14	C13	115.91(10)
N3	S3	O2	108.38(5)	C12	C13	C14	118.81(11)
C9	S3	O1	104.01(5)	C11	C12	C13	120.35(11)
C9	S3	O2	108.43(5)	C10	C11	C12	119.98(11)
C9	S3	N3	109.33(5)	C11	C10	C9	120.72(11)
C3	C4	C5	120.14(12)	O4	N4	O3	124.87(12)
C6	C5	C4	118.81(13)	C14	N4	O3	116.97(10)
C1	C6	C5	122.15(12)	C14	N4	O4	118.06(11)
N5	C6	C5	116.24(11)	C22	C21	C20	118.31(13)
N5	C6	C1	121.59(11)	C21	C22	C17	122.72(12)
C6	C1	S1	124.12(9)	N1	C22	C17	120.48(11)
C2	C1	S1	117.67(10)	N1	C22	C21	116.80(11)
C2	C1	C6	118.19(11)	O8	N1	O7	125.20(12)
C7	N6	S1	118.28(8)	C22	N1	O7	117.80(11)
C8	C7	N6	110.42(9)	C22	N1	O8	116.96(11)
N3	C8	C7	113.76(9)	C3	C2	C1	119.86(13)
C8	N3	S3	117.69(8)	C2	C3	C4	120.81(12)
C15	N3	S3	121.14(8)	O12	N5	O11	123.59(12)
C15	N3	C8	119.46(9)	C6	N5	O11	117.49(11)
C16	C15	N3	111.53(9)	C6	N5	O12	118.84(10)

## CONCLUSIONS

We have produced a library of chelidamic acid derivatives and determined their crystallographic structures using XRD analysis. In addition, the Ns-DETA solid-state structure was obtained. Overall, these results will assist in determining electronic effects on structure, electrochemistry and reactivity in biological and catalysis activity that the Green Research Group is currently exploring.

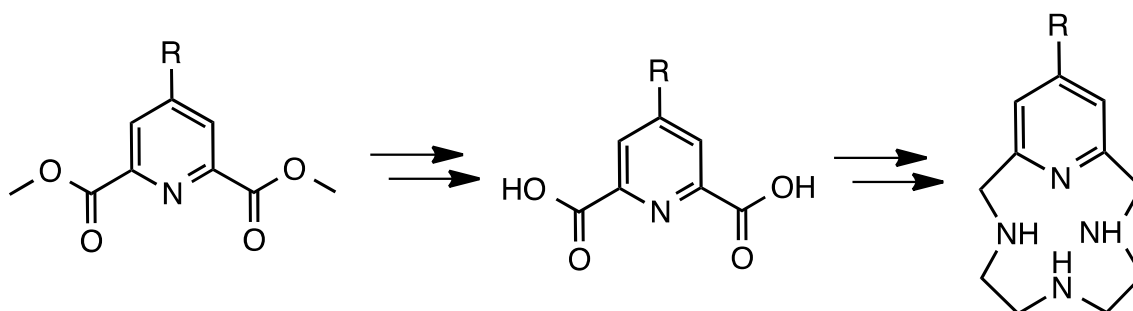


**Figure 13.** Future synthesis pathway of the Green Research Group.

The Green Research Group is interested in continuing to evaluate the electronics of the various functionalization of the pyridol core of the chelidamic acid congeners. The functionalization will continue to undergo experimentation to determine the functional groups with greatest efficacy as potential therapeutic agents for Alzheimer's Disease. Future experimentation will follow the synthetic pathway broadly delineated in **Figure 13** and will represent a variety of functional groups.

## SUPPORTING MATERIALS

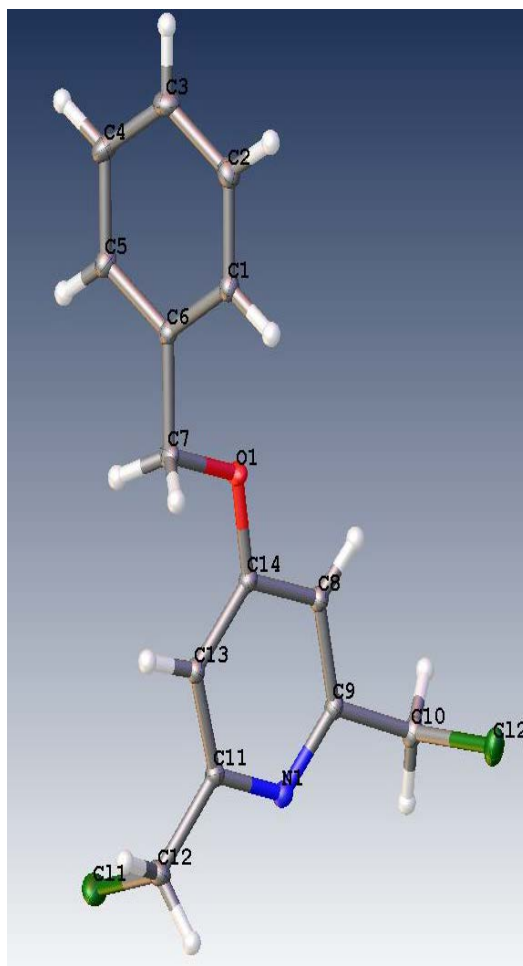


**Figure S1.** Thermal ellipsoid (50%) plot of **2** with labeling schemes adopted.

**Table S1.1.** Hydrogen bond distances (Å) and angles (°) for **2**.

<b>Atom</b>	<b>Donor-H</b>	<b>Acceptor-H</b>	<b>Donor-Acceptor</b>	<b>Angle</b>
C12-H12...N1	0.99	2.66	3.4944(9)	142.2
C12-H12'...O1	0.99	2.61	3.5147(9)	151.5
C10-H10...Cl1	0.99	2.88	3.7003(8)	140.8
C10-H10...Cl1	0.99	2.88	3.7003(8)	140.8
C12-H12'...O1	0.99	2.61	3.5147(9)	151.5
C12-H12...N1	0.99	2.66	3.4944(9)	142.2

**Table S1.2.** Atomic coordinates and equivalent isotropic atomic displacement parameters ( $\text{\AA}^2$ ) for **2**.

<b>Atom</b>	<b>x/a</b>	<b>y/b</b>	<b>z/c</b>	<b>U(eq)</b>
Cl1	0.69080(2)	0.91290(3)	0.98936(2)	0.02192(5)
Cl2	0.41883(2)	0.05082(2)	0.34636(2)	0.01981(5)
O1	0.82887(4)	0.16671(6)	0.46452(4)	0.01265(9)
N1	0.58056(4)	0.99625(7)	0.18453(5)	0.01153(9)
C3	0.13186(5)	0.38275(9)	0.77877(6)	0.01713(12)
C2	0.03396(6)	0.45276(9)	0.74744(6)	0.01614(12)
C1	0.96089(5)	0.41811(9)	0.63905(6)	0.01364(11)
C6	0.98502(5)	0.31226(8)	0.56153(5)	0.01131(10)
C7	0.90579(5)	0.27401(9)	0.44515(5)	0.01334(11)
C14	0.75009(5)	0.11578(8)	0.36921(5)	0.01033(10)
C8	0.67112(5)	0.02797(8)	0.38978(5)	0.01136(10)
C9	0.58776(5)	0.97423(8)	0.29530(5)	0.01077(10)
C10	0.49767(5)	0.89214(8)	0.31414(6)	0.01405(11)
C12	0.64769(5)	0.10009(9)	0.04159(6)	0.01521(11)
C11	0.65773(5)	0.07848(8)	0.16620(5)	0.01087(10)
C4	0.15703(5)	0.27982(9)	0.70144(6)	0.01679(12)
C5	0.08349(5)	0.24408(9)	0.59298(6)	0.01410(11)
C13	0.74281(5)	0.14376(8)	0.25440(5)	0.01141(10)

**Table S1.3.** Bond lengths (Å) for **2**.

C11-C12	1.8055(8)	C12-C10	1.8043(7)
O1-C14	1.3561(7)	O1-C7	1.4514(8)
N1-C11	1.3411(8)	N1-C9	1.3421(8)
C3-C4	1.3895(11)	C3-C2	1.3940(10)
C3-H3	0.95	C2-C1	1.3917(10)
C2-H2	0.95	C1-C6	1.3981(9)
C1-H1	0.95	C6-C5	1.3952(9)
C6-C7	1.5003(9)	C7-H7	0.99
C7-H7'	0.99	C14-C8	1.3968(9)
C14-C13	1.3977(9)	C8-C9	1.3903(9)
C8-H8	0.95	C9-C10	1.5005(9)
C10-H10	0.99	C10-H10'	0.99
C12-C11	1.4994(9)	C12-H12'	0.99
C12-H12	0.99	C11-C13	1.3954(9)
C4-C5	1.3967(9)	C4-H4	0.95
C5-H5	0.95	C13-H13	0.95

**Table S1.4.** Bond angles (°) for **2**.

C14-O1-C7	116.88(5)	C11-N1-C9	117.03(5)
C4-C3-C2	120.11(6)	C4-C3-H3	119.9
C2-C3-H3	119.9	C1-C2-C3	120.01(6)
C1-C2-H2	120.0	C3-C2-H2	120.0
C2-C1-C6	120.25(6)	C2-C1-H1	119.9
C6-C1-H1	119.9	C5-C6-C1	119.43(6)
C5-C6-C7	120.45(6)	C1-C6-C7	120.11(6)
O1-C7-C6	107.43(5)	O1-C7-H7	110.2
C6-C7-H7	110.2	O1-C7-H7'	110.2
C6-C7-H7'	110.2	H7-C7-H7'	108.5
O1-C14-C8	116.16(5)	O1-C14-C13	125.22(5)
C8-C14-C13	118.62(5)	C9-C8-C14	118.70(6)

C9-C8-H8	120.6	C14-C8-H8	120.6
N1-C9-C8	123.54(6)	N1-C9-C10	116.35(5)
C8-C9-C10	120.08(6)	C9-C10-Cl2	109.45(5)
C9-C10-H10	109.8	Cl2-C10-H10	109.8
C9-C10-H10'	109.8	Cl2-C10-H10'	109.8
H10-C10-H10'	108.2	C11-C12-Cl1	110.20(5)
C11-C12-H12'	109.6	Cl1-C12-H12'	109.6
C11-C12-H12	109.6	Cl1-C12-H12	109.6
H12'-C12-H12	108.1	N1-C11-C13	124.12(6)
N1-C11-C12	115.72(5)	C13-C11-C12	120.16(6)
C3-C4-C5	119.89(6)	C3-C4-H4	120.1
C5-C4-H4	120.1	C6-C5-C4	120.30(6)
C6-C5-H5	119.8	C4-C5-H5	119.8
C11-C13-C14	117.91(6)	C11-C13-H13	121.0
C14-C13-H13	121.0		

**Table S1.5.** Torsion angles (°) for **2**.

C4-C3-C2-C1	0.72(11)	C3-C2-C1-C6	0.43(11)
C2-C1-C6-C5	-1.11(10)	C2-C1-C6-C7	179.48(6)
C14-O1-C7-C6	-179.36(5)	C5-C6-C7-O1	110.00(7)
C1-C6-C7-O1	-70.60(8)	C7-O1-C14-C8	-173.31(6)
C7-O1-C14-C13	6.98(9)	O1-C14-C8-C9	179.30(6)
C13-C14-C8-C9	-0.97(9)	C11-N1-C9-C8	-1.68(9)
C11-N1-C9-C10	176.11(6)	C14-C8-C9-N1	2.72(10)
C14-C8-C9-C10	-174.99(6)	N1-C9-C10-Cl2	-100.12(6)
C8-C9-C10-Cl2	77.75(7)	C9-N1-C11-C13	-1.10(9)
C9-N1-C11-C12	179.65(6)	Cl1-C12-C11-N1	-82.66(6)
Cl1-C12-C11-C13	98.06(6)	C2-C3-C4-C5	-1.17(11)
C1-C6-C5-C4	0.66(10)	C7-C6-C5-C4	-179.94(6)
C3-C4-C5-C6	0.47(11)	N1-C11-C13-C14	2.70(10)
C12-C11-C13-C14	-178.08(6)	O1-C14-C13-C11	178.17(6)
C8-C14-C13-C11	-1.53(9)		

**Table S1.6.** Anisotropic atomic displacement parameters ( $\text{\AA}^2$ ) for **2**.

Atom	U11	U22	U33	U23	U13	U12
Cl1	0.01841(8)	0.03071(10)	0.01642(8)	-0.00943(6)	0.00583(6)	-0.00032(6)
Cl2	0.01515(8)	0.02363(9)	0.02377(9)	0.00283(6)	0.01070(6)	0.00340(5)
O1	0.01080(18)	0.0163(2)	0.00982(18)	-0.00077(15)	0.00233(14)	-0.00501(15)
N1	0.0105(2)	0.0114(2)	0.0121(2)	-0.00039(16)	0.00319(16)	-0.00065(16)
C3	0.0160(3)	0.0193(3)	0.0128(3)	-0.0010(2)	0.0008(2)	-0.0029(2)
C2	0.0171(3)	0.0181(3)	0.0137(3)	-0.0032(2)	0.0060(2)	-0.0024(2)
C1	0.0116(2)	0.0154(3)	0.0144(3)	-0.0010(2)	0.0052(2)	-0.00042(19)
C6	0.0100(2)	0.0125(2)	0.0110(2)	0.00010(18)	0.00305(18)	-0.00208(18)
C7	0.0110(2)	0.0171(3)	0.0112(2)	0.00013(19)	0.00300(18)	-0.00460(19)
C14	0.0093(2)	0.0109(2)	0.0103(2)	-0.00078(17)	0.00282(18)	-0.00104(17)
C8	0.0110(2)	0.0122(2)	0.0111(2)	0.00001(18)	0.00403(18)	-0.00160(18)
C9	0.0095(2)	0.0099(2)	0.0129(2)	-0.00007(18)	0.00383(18)	-0.00075(17)
C10	0.0117(2)	0.0138(2)	0.0172(3)	0.0001(2)	0.0057(2)	-0.00252(19)
C12	0.0161(3)	0.0185(3)	0.0105(2)	0.0006(2)	0.0039(2)	-0.0012(2)
C11	0.0105(2)	0.0113(2)	0.0104(2)	-0.00001(17)	0.00307(18)	0.00003(17)
C4	0.0116(2)	0.0174(3)	0.0178(3)	0.0001(2)	0.0007(2)	0.0006(2)
C5	0.0118(2)	0.0141(2)	0.0157(3)	-0.0018(2)	0.0040(2)	-0.00014(19)
C13	0.0106(2)	0.0131(2)	0.0106(2)	-0.00027(18)	0.00379(18)	-0.00156(18)

**Table S1.7.** Hydrogen atomic coordinates and isotropic atomic displacement parameters ( $\text{\AA}^2$ ) for **2**.

<b>Atom</b>	<b>x/a</b>	<b>y/b</b>	<b>z/c</b>	<b>U(eq)</b>
H3	1.1814	0.4054	0.8531	0.021
H2	1.0171	0.5241	0.8001	0.019
H1	0.8944	0.4666	0.6177	0.016
H7	0.8738	0.3793	0.4062	0.016
H7'	0.9379	0.2161	0.3953	0.016
H8	0.6743	0.0054	0.4668	0.014
H10	0.5222	-0.1885	0.3794	0.017
H10'	0.4567	-0.1706	0.2436	0.017
H12'	0.6893	0.1975	0.0342	0.018
H12	0.5751	0.1226	-0.0060	0.018
H4	1.2242	0.2338	0.7223	0.02
H5	1.1006	0.1730	0.5404	0.017
H13	0.7942	0.2053	0.2370	0.014

**Table S2.1.** Fractional Atomic Coordinates ( $\times 10^4$ ) and Equivalent Isotropic Displacement Parameters ( $\text{\AA}^2 \times 10^3$ ) for **3**.

Atom	x	y	z	U(eq)
S1	8761.81(17)	-1182.8(2)	4938.2(3)	15.19(7)
S2	5661.10(17)	2294.9(2)	3728.5(2)	15.20(7)
S3	8423.37(16)	2740.8(2)	6100.0(2)	10.76(6)
O1	8766.6(5)	1897.1(7)	6753.7(7)	15.27(16)
O2	7680.8(5)	3161.1(7)	6360.4(7)	15.27(16)
O3	7966.6(6)	4848.3(8)	4720.2(8)	21.32(19)
O4	7869.8(7)	5975.0(9)	6041.7(10)	30.7(2)
O13	5154.1(6)	2457.1(9)	2791.5(8)	20.97(19)
O7	6379.6(6)	3904.4(8)	2073.3(8)	23.8(2)
O8	5387.3(7)	4988.8(9)	2023.4(9)	27.3(2)
O9	8918.6(6)	-1718.2(8)	5947.6(8)	22.01(19)
O10	9125.6(6)	-1553.4(8)	3991.3(9)	23.5(2)
O11	7034.1(7)	-1320.1(10)	7232.9(9)	28.8(2)
O12	7879.7(6)	-163.5(8)	6735.1(8)	21.56(19)
C4	6155.7(8)	-1366.3(12)	4061.5(12)	24.2(3)
C5	6391.0(8)	-1172.2(11)	5131.7(12)	21.6(2)
C6	7177.2(7)	-1103.9(9)	5401.7(10)	15.1(2)
C1	7743.0(7)	-1240.1(9)	4633.9(10)	14.09(19)
N6	9000.6(6)	63.5(8)	5081.3(8)	14.14(17)
C7	9050.8(7)	723.4(9)	4103.7(9)	14.23(19)
C8	9081.4(7)	1908.1(9)	4400.4(9)	13.21(19)

N3	8364.3(6)	2308.6(8)	4867.9(8)	12.51(17)
C15	7682.3(6)	2547.3(9)	4149.2(9)	12.68(18)
C16	7117.1(7)	1600.1(10)	4076.9(11)	16.9(2)
N2	6468.8(6)	1826.9(9)	3301.9(9)	16.20(18)
C17	5851.5(7)	3573.2(10)	4311.5(10)	15.5(2)
C18	5882.3(7)	3673.8(11)	5432(1)	18.8(2)
C19	5991.4(8)	4679.6(12)	5911.8(11)	22.1(2)
C20	6043.8(8)	5588.4(12)	5275.8(12)	22.4(2)
C9	9120.3(7)	3799.1(9)	6207.3(9)	11.78(18)
C14	8956.3(7)	4886.4(9)	6032.9(9)	13.81(19)
C13	9507.6(8)	5677.2(10)	6242.2(10)	18.1(2)
C12	10257.8(8)	5374.9(11)	6583.5(11)	19.5(2)
C11	10441.4(7)	4298.6(10)	6739.6(10)	16.6(2)
C10	9869.6(7)	3519.7(9)	6577.7(9)	13.45(19)
N4	8199.6(6)	5254.7(8)	5574.8(9)	17.23(19)
C21	5995.0(8)	5511.4(11)	4153.9(11)	20.2(2)
C22	5914.1(7)	4507.7(10)	3694.3(10)	16.3(2)
N1	5886.5(7)	4454.4(9)	2505.1(9)	18.8(2)
C2	7496.8(8)	-1457.2(10)	3572.1(11)	19.2(2)
C3	6701.4(8)	-1509.2(11)	3291.3(12)	22.9(3)
N5	7388.1(6)	-853.2(9)	6535.3(9)	17.52(19)
O14	5434.7(6)	1622.4(9)	4592.8(8)	22.38(19)

**Table S2.2.** Anisotropic Displacement Parameters ( $\text{\AA}^2 \times 10^3$ ) for **3**.

Atom	U11	U22	U33	U12	U13	U23
S1	12.04(12)	10.74(12)	22.72(14)	2.63(9)	0.11(10)	-2.04(9)
S2	10.27(12)	17.84(14)	17.25(13)	-1.84(9)	-2.08(9)	1.69(10)
S3	10.75(11)	10.89(11)	10.64(11)	-0.19(8)	0.44(8)	0.15(8)
O1	17.9(4)	12.7(4)	14.9(4)	0.2(3)	-1.8(3)	3.5(3)
O2	12.0(4)	17.3(4)	16.7(4)	1.2(3)	3.1(3)	-1.4(3)
O3	22.9(5)	20.2(4)	20.2(4)	0.8(3)	-6.5(3)	0.2(3)
O4	25.2(5)	26.0(5)	40.5(6)	10.6(4)	-2.9(5)	-13.3(5)
O13	14.7(4)	25.4(5)	22.0(4)	-1.5(3)	-7.5(3)	1.3(4)
O7	28.6(5)	23.2(5)	20.2(4)	1.5(4)	6.9(4)	-1.0(4)
O8	28.9(5)	27.2(5)	25.2(5)	4.3(4)	-7.2(4)	7.1(4)
O9	20.5(4)	14.7(4)	30.1(5)	2.6(3)	-6.3(4)	4.8(4)
O10	19.1(4)	20.3(4)	31.6(5)	4.3(3)	5.6(4)	-10.6(4)
O11	32.5(6)	31.6(6)	22.7(5)	-9.9(4)	6.6(4)	7.5(4)
O12	19.0(4)	26.6(5)	19.2(4)	-7.7(4)	1.9(3)	-2.1(4)
C4	16.6(6)	24.4(6)	30.9(7)	-0.5(5)	-8.5(5)	-3.1(5)
C5	13.6(5)	23.7(6)	27.3(6)	-2.1(4)	0.4(4)	-1.3(5)
C6	13.7(5)	13.8(5)	17.6(5)	-1.5(4)	-0.0(4)	1.1(4)
C1	14.0(5)	9.8(4)	18.4(5)	0.7(3)	-0.1(4)	0.3(4)
N6	13.8(4)	12.7(4)	16.0(4)	-0.7(3)	1.2(3)	-1.5(3)
C7	13.8(5)	15.0(5)	14.0(4)	1.4(4)	2.7(4)	-2.1(4)
C8	11.3(4)	13.8(4)	14.7(4)	0.5(4)	2.6(3)	-0.4(4)

N3	10.2(4)	15.4(4)	11.8(4)	2.4(3)	-1.3(3)	-2.4(3)
C15	11.1(4)	12.7(4)	14.0(4)	-0.0(3)	-2.3(4)	-0.0(4)
C16	12.7(5)	13.2(5)	24.3(6)	-0.3(4)	-4.6(4)	1.8(4)
N2	12.8(4)	18.3(4)	17.2(4)	0.1(3)	-3.1(3)	-2.8(4)
C17	10.2(4)	19.2(5)	17.0(5)	2.3(4)	0.5(4)	1.1(4)
C18	15.4(5)	24.3(6)	16.6(5)	3.1(4)	0.6(4)	0.8(4)
C19	18.8(6)	29.9(7)	17.6(5)	4.6(5)	0.3(4)	-4.2(5)
C20	18.8(6)	23.9(6)	24.6(6)	4.5(5)	0.9(5)	-7.3(5)
C9	12.5(4)	11.7(4)	11.0(4)	-0.8(3)	-0.1(3)	-1.5(3)
C14	15.2(5)	12.5(4)	13.6(4)	1.1(4)	-1.0(4)	-0.8(4)
C13	23.1(6)	11.7(5)	19.3(5)	-2.9(4)	-1.8(4)	-1.3(4)
C12	20.6(6)	18.3(5)	19.3(5)	-7.0(4)	-3.3(4)	-1.6(4)
C11	13.6(5)	20.3(5)	15.6(5)	-3.2(4)	-2.3(4)	-1.2(4)
C10	13.0(5)	14.1(4)	13.2(4)	0.0(4)	0.0(3)	-1.1(4)
N4	17.3(5)	12.4(4)	21.8(5)	1.9(3)	-0.7(4)	0.1(4)
C21	19.0(5)	18.6(5)	23.1(6)	2.3(4)	1.9(4)	-1.4(5)
C22	14.0(5)	18.9(5)	16.0(5)	2.5(4)	1.4(4)	-0.2(4)
N1	21.1(5)	17.9(5)	17.3(5)	-1.3(4)	-0.9(4)	2.0(4)
C2	22.1(6)	16.7(5)	18.6(5)	2.2(4)	-1.3(4)	-2.9(4)
C3	24.0(6)	21.0(6)	22.9(6)	1.6(5)	-8.7(5)	-3.4(5)
N5	15.9(4)	18.5(5)	18.2(4)	-1.4(4)	1.9(4)	2.9(4)
O14	18.7(4)	25.0(5)	23.4(4)	-5.9(4)	0.8(3)	5.8(4)

**Table S2.3.** Hydrogen Atom Coordinates ( $\text{\AA}\times 10^4$ ) and Isotropic Displacement Parameters ( $\text{\AA}^2\times 10^3$ ) for **3**.

Atom	x	y	z	U(eq)
H4	8109(8)	6104(14)	6636(9)	46.0(4)
H11	6936(13)	-1951(6)	7029(9)	43.2(4)
H12	8234(6)	-210(11)	6289(11)	32.3(3)
H4a	5616.3(8)	-1400.8(12)	3858.5(12)	29.1(3)
H5	6017.5(8)	-1087.6(11)	5670.4(12)	25.9(3)
H6	9098.2(6)	339.9(8)	5729.7(8)	17.0(2)
H7a	9524.1(7)	526.8(9)	3719.8(9)	17.1(2)
H7b	8591.9(7)	585.3(9)	3609.4(9)	17.1(2)
H8a	9523.7(7)	2028.2(9)	4928.7(9)	15.8(2)
H8b	9182.0(7)	2329.8(9)	3741.0(9)	15.8(2)
H15a	7410.2(6)	3185.0(9)	4425.7(9)	15.2(2)
H15b	7856.4(6)	2719.2(9)	3414.9(9)	15.2(2)
H16a	7396.1(7)	949.4(10)	3845.7(11)	20.3(3)
H16b	6913.0(7)	1459.1(10)	4801.1(11)	20.3(3)
H2	6518.7(6)	1708.6(9)	2605.2(9)	19.4(2)
H18	5828.9(7)	3055.9(11)	5873.9(10)	22.6(3)
H19	6029.9(8)	4740.6(12)	6679.9(11)	26.5(3)
H20	6113.8(8)	6270.8(12)	5610.1(12)	26.9(3)
H13	9376.0(8)	6413.9(10)	6154.3(10)	21.7(3)
H12a	10647.1(8)	5907.5(11)	6710.8(11)	23.4(3)
H11a	10958.0(7)	4095.1(10)	6957(1)	19.9(3)
H10	9991.6(7)	2788.0(9)	6721.5(9)	16.1(2)
H21	6016.8(8)	6135.3(11)	3713.2(11)	24.2(3)
H2a	7868.4(8)	-1570.5(10)	3036.1(11)	23.0(3)
H3	6535.0(8)	-1644.9(11)	2559.4(12)	27.5(3)

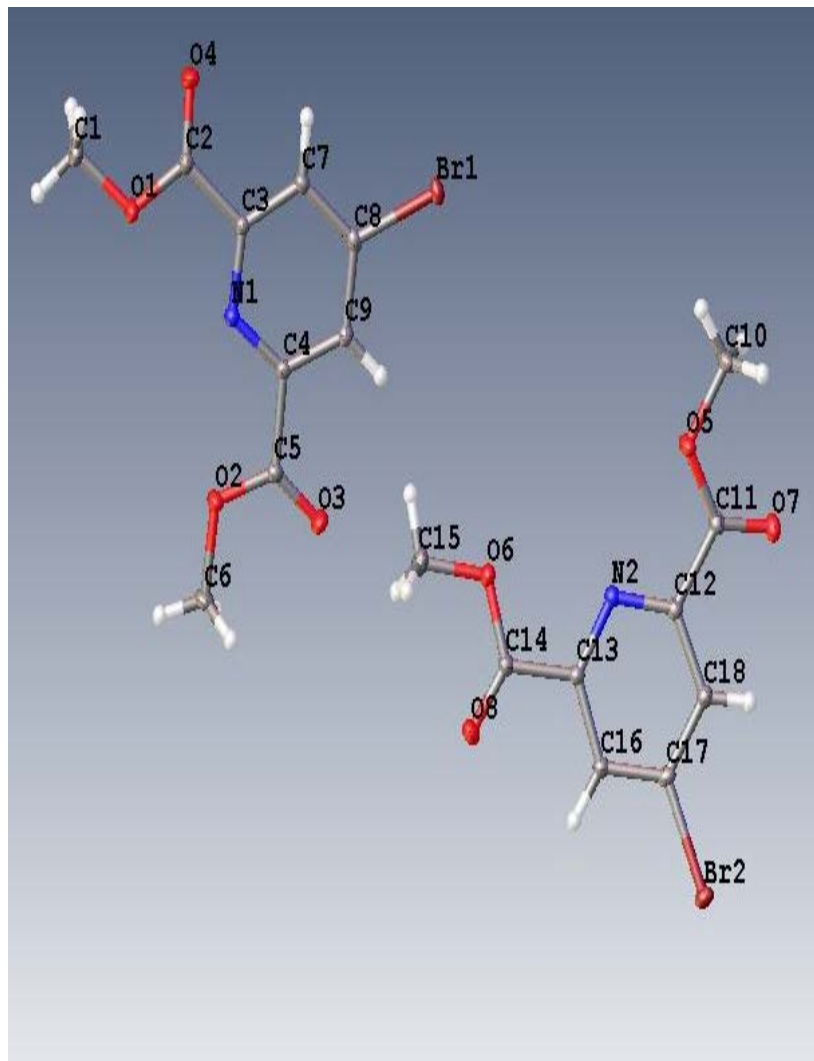


**Figure S2.** Thermal ellipsoid (50%) plot of **4** with labeling schemes adopted.

**Table S3.1.** Atomic coordinates and equivalent isotropic atomic displacement parameters ( $\text{\AA}^2$ ) for **4**.

	<b>x/a</b>	<b>y/b</b>	<b>z/c</b>	<b>U(eq)</b>
Br1	0.19736(4)	0.45189(2)	0.21773(2)	0.01461(3)
Br2	0.51836(4)	0.07005(2)	0.71211(2)	0.01651(4)
O1	0.3038(3)	0.27114(8)	0.91718(6)	0.0197(2)
O2	0.2594(3)	0.03969(8)	0.07251(6)	0.0174(2)
O3	0.5771(3)	0.06728(9)	0.17864(6)	0.0209(2)
O4	0.6455(4)	0.41908(9)	0.93977(7)	0.0251(3)
O5	0.1059(3)	0.45321(8)	0.57014(6)	0.0174(2)
O6	0.4135(3)	0.22160(8)	0.40208(6)	0.01629(19)
O7	0.3339(3)	0.40842(8)	0.67111(6)	0.0179(2)
O8	0.1132(3)	0.08296(9)	0.43148(7)	0.0217(2)
N1	0.5026(3)	0.22082(8)	0.04279(6)	0.01180(19)
N2	0.7359(3)	0.27082(8)	0.53294(6)	0.01205(19)
C1	0.2124(5)	0.29429(13)	0.84617(9)	0.0218(3)
C2	0.5278(4)	0.34139(10)	0.95847(8)	0.0140(2)
C3	0.6221(3)	0.31323(10)	0.03053(7)	0.0118(2)
C4	0.5990(3)	0.19795(10)	0.10694(7)	0.0116(2)
C5	0.4786(4)	0.09449(10)	0.12361(8)	0.0135(2)
C6	0.1365(4)	0.93872(10)	0.08578(9)	0.0181(3)
C7	0.8326(3)	0.38540(10)	0.07991(8)	0.0132(2)
C8	0.9233(3)	0.35934(10)	0.14630(7)	0.0124(2)
C9	0.8081(4)	0.26375(10)	0.16057(7)	0.0130(2)
C10	0.3217(4)	0.55008(11)	0.58702(9)	0.0200(3)
C11	0.1369(4)	0.39102(10)	0.61762(8)	0.0130(2)
C12	0.8928(3)	0.29458(10)	0.59921(7)	0.0118(2)
C13	0.5204(3)	0.18414(10)	0.51953(7)	0.0119(2)
C14	0.3277(4)	0.15615(10)	0.44664(7)	0.0131(2)
C15	0.2210(4)	0.20066(12)	0.33240(8)	0.0201(3)
C16	0.4511(4)	0.11946(10)	0.57003(8)	0.0130(2)
C17	0.6142(4)	0.14814(10)	0.63866(8)	0.0134(2)
C18	0.8422(4)	0.23640(10)	0.65413(8)	0.0137(2)

**Table S3.2.** Bond lengths (Å) for **4**.

Br1-C8	1.8818(13)	Br2-C17	1.8822(13)
O1-C2	1.3346(17)	O1-C1	1.4507(19)
O2-C5	1.3249(17)	O2-C6	1.4558(17)
O3-C5	1.2088(17)	O4-C2	1.2044(17)
O5-C11	1.3268(17)	O5-C10	1.4536(18)
O6-C14	1.3311(17)	O6-C15	1.4474(19)
O7-C11	1.2113(17)	O8-C14	1.2071(17)
N1-C4	1.3348(18)	N1-C3	1.3395(17)
N2-C12	1.3344(18)	N2-C13	1.3420(17)
C1-H6	0.98	C1-H7	0.98
C1-H1	0.98	C2-C3	1.4993(19)
C3-C7	1.3956(19)	C4-C9	1.3952(19)
C4-C5	1.5069(18)	C6-H2	0.98
C6-H8	0.98	C6-H3	0.98
C7-C8	1.385(2)	C7-H5	0.95
C8-C9	1.3882(19)	C9-H4	0.95
C10-H11	0.98	C10-H9	0.98
C10-H16	0.98	C11-C12	1.5048(19)
C12-C18	1.3944(19)	C13-C16	1.3971(18)
C13-C14	1.501(2)	C15-H12	0.98
C15-H13	0.98	C15-H10	0.98
C16-C17	1.386(2)	C16-H15	0.95
C17-C18	1.3850(19)	C18-H14	0.95

**Table S3.3.** Bond angles (°) for **4**.

C2-O1-C1	114.83(12)	C5-O2-C6	115.17(11)
C11-O5-C10	115.45(12)	C14-O6-C15	114.82(11)
C4-N1-C3	116.19(12)	C12-N2-C13	116.43(12)
O1-C1-H6	109.5	O1-C1-H7	109.5
H6-C1-H7	109.5	O1-C1-H1	109.5
H6-C1-H1	109.5	H7-C1-H1	109.5
O4-C2-O1	123.74(14)	O4-C2-C3	123.20(13)
O1-C2-C3	113.05(11)	N1-C3-C7	124.65(12)
N1-C3-C2	118.07(12)	C7-C3-C2	117.27(11)
N1-C4-C9	124.32(12)	N1-C4-C5	118.85(12)
C9-C4-C5	116.83(12)	O3-C5-O2	125.33(13)
O3-C5-C4	121.71(13)	O2-C5-C4	112.96(12)
O2-C6-H2	109.5	O2-C6-H8	109.5
H2-C6-H8	109.5	O2-C6-H3	109.5
H2-C6-H3	109.5	H8-C6-H3	109.5
C8-C7-C3	117.46(12)	C8-C7-H5	121.3
C3-C7-H5	121.3	C7-C8-C9	119.51(12)
C7-C8-Br1	121.02(10)	C9-C8-Br1	119.47(10)
C8-C9-C4	117.85(12)	C8-C9-H4	121.1
C4-C9-H4	121.1	O5-C10-H11	109.5
O5-C10-H9	109.5	H11-C10-H9	109.5
O5-C10-H16	109.5	H11-C10-H16	109.5
H9-C10-H16	109.5	O7-C11-O5	125.04(13)
O7-C11-C12	122.17(13)	O5-C11-C12	112.78(12)
N2-C12-C18	124.28(13)	N2-C12-C11	118.94(12)
C18-C12-C11	116.78(12)	N2-C13-C16	124.40(13)
N2-C13-C14	118.35(12)	C16-C13-C14	117.20(12)
O8-C14-O6	124.36(13)	O8-C14-C13	122.80(13)
O6-C14-C13	112.82(11)	O6-C15-H12	109.5
O6-C15-H13	109.5	H12-C15-H13	109.5
O6-C15-H10	109.5	H12-C15-H10	109.5
H13-C15-H10	109.5	C17-C16-C13	117.22(12)
C17-C16-H15	121.4	C13-C16-H15	121.4
C18-C17-C16	119.96(12)	C18-C17-Br2	119.51(11)
C16-C17-Br2	120.50(10)	C17-C18-C12	117.69(13)
C17-C18-H14	121.2	C12-C18-H14	121.2

**Table S3.4.** Torsion angles (°) for **4**.

C1-O1-C2-O4	0.8(2)	C1-O1-C2-C3	-178.47(13)
C4-N1-C3-C7	-0.8(2)	C4-N1-C3-C2	178.47(12)
O4-C2-C3-N1	-173.35(15)	O1-C2-C3-N1	5.96(19)
O4-C2-C3-C7	5.9(2)	O1-C2-C3-C7	-174.74(13)
C3-N1-C4-C9	0.8(2)	C3-N1-C4-C5	-178.89(12)
C6-O2-C5-O3	-0.6(2)	C6-O2-C5-C4	179.65(12)
N1-C4-C5-O3	174.73(14)	C9-C4-C5-O3	-5.0(2)
N1-C4-C5-O2	-5.52(19)	C9-C4-C5-O2	174.78(13)
N1-C3-C7-C8	-0.1(2)	C2-C3-C7-C8	-179.34(13)
C3-C7-C8-C9	1.0(2)	C3-C7-C8-Br1	-178.52(10)
C7-C8-C9-C4	-1.0(2)	Br1-C8-C9-C4	178.54(10)
N1-C4-C9-C8	0.1(2)	C5-C4-C9-C8	179.73(13)
C10-O5-C11-O7	-2.1(2)	C10-O5-C11-C12	176.75(12)
C13-N2-C12-C18	-1.0(2)	C13-N2-C12-C11	-179.83(12)
O7-C11-C12-N2	-166.01(14)	O5-C11-C12-N2	15.06(18)
O7-C11-C12-C18	15.1(2)	O5-C11-C12-C18	-163.87(13)
C12-N2-C13-C16	0.5(2)	C12-N2-C13-C14	177.70(12)
C15-O6-C14-O8	1.6(2)	C15-O6-C14-C13	-176.83(12)
N2-C13-C14-O8	-175.20(14)	C16-C13-C14-O8	2.2(2)
N2-C13-C14-O6	3.28(19)	C16-C13-C14-O6	-179.33(12)
N2-C13-C16-C17	0.8(2)	C14-C13-C16-C17	-176.40(12)
C13-C16-C17-C18	-1.7(2)	C13-C16-C17-Br2	176.39(10)
C16-C17-C18-C12	1.3(2)	Br2-C17-C18-C12	-176.82(10)
N2-C12-C18-C17	0.1(2)	C11-C12-C18-C17	178.97(12)

**Table S3.5.** Anisotropic atomic displacement parameters ( $\text{\AA}^2$ ) for **4**.

	<b>U11</b>	<b>U22</b>	<b>U33</b>	<b>U23</b>	<b>U13</b>	<b>U12</b>
Br1	0.01397(6)	0.01394(6)	0.01368(6)	-0.00119(4)	-0.00207(4)	-0.00129(4)
Br2	0.01839(7)	0.01709(6)	0.01521(6)	0.00786(5)	0.00164(5)	0.00067(5)
O1	0.0261(5)	0.0153(4)	0.0152(5)	0.0053(4)	-0.0082(4)	-0.0053(4)
O2	0.0216(5)	0.0121(4)	0.0167(5)	0.0045(4)	-0.0041(4)	-0.0042(4)
O3	0.0283(6)	0.0173(5)	0.0161(5)	0.0078(4)	-0.0056(4)	-0.0030(4)
O4	0.0338(7)	0.0192(5)	0.0195(5)	0.0096(4)	-0.0056(5)	-0.0105(5)
O5	0.0192(5)	0.0123(4)	0.0193(5)	0.0055(4)	-0.0053(4)	-0.0033(4)
O6	0.0183(5)	0.0160(4)	0.0134(4)	0.0051(4)	-0.0028(4)	-0.0028(4)
O7	0.0198(5)	0.0155(4)	0.0170(5)	0.0017(4)	-0.0057(4)	0.0007(4)
O8	0.0253(6)	0.0182(5)	0.0180(5)	0.0030(4)	-0.0025(4)	-0.0087(4)
N1	0.0126(5)	0.0106(4)	0.0119(5)	0.0026(4)	0.0000(4)	-0.0002(4)
N2	0.0128(5)	0.0107(4)	0.0125(5)	0.0023(4)	0.0002(4)	0.0009(4)
C1	0.0268(7)	0.0216(7)	0.0159(6)	0.0049(5)	-0.0061(6)	-0.0005(6)
C2	0.0158(6)	0.0127(5)	0.0127(5)	0.0025(4)	-0.0008(4)	-0.0011(4)
C3	0.0129(5)	0.0104(5)	0.0115(5)	0.0026(4)	-0.0001(4)	-0.0004(4)
C4	0.0124(5)	0.0102(5)	0.0120(5)	0.0025(4)	0.0010(4)	0.0001(4)
C5	0.0154(5)	0.0115(5)	0.0134(5)	0.0026(4)	0.0010(4)	0.0001(4)
C6	0.0212(6)	0.0104(5)	0.0214(7)	0.0039(5)	-0.0007(5)	-0.0031(5)
C7	0.0135(5)	0.0111(5)	0.0137(5)	0.0014(4)	0.0000(4)	-0.0014(4)
C8	0.0113(5)	0.0121(5)	0.0128(5)	-0.0001(4)	0.0008(4)	0.0003(4)
C9	0.0136(5)	0.0130(5)	0.0122(5)	0.0021(4)	-0.0001(4)	0.0009(4)
C10	0.0208(7)	0.0130(6)	0.0245(7)	0.0049(5)	-0.0038(5)	-0.0047(5)
C11	0.0139(5)	0.0112(5)	0.0136(5)	0.0011(4)	0.0003(4)	0.0021(4)
C12	0.0120(5)	0.0107(5)	0.0130(5)	0.0023(4)	0.0003(4)	0.0021(4)
C13	0.0127(5)	0.0109(5)	0.0120(5)	0.0023(4)	0.0011(4)	0.0012(4)
C14	0.0147(5)	0.0118(5)	0.0125(5)	0.0022(4)	0.0008(4)	0.0006(4)
C15	0.0219(7)	0.0225(7)	0.0151(6)	0.0056(5)	-0.0036(5)	-0.0004(5)
C16	0.0142(5)	0.0113(5)	0.0136(5)	0.0030(4)	0.0011(4)	0.0009(4)
C17	0.0135(5)	0.0136(5)	0.0145(5)	0.0057(4)	0.0024(4)	0.0030(4)
C18	0.0143(5)	0.0142(5)	0.0129(5)	0.0038(4)	0.0004(4)	0.0019(4)

**Table S3.6.** Hydrogen atomic coordinates and isotropic atomic displacement parameters ( $\text{\AA}^2$ ) for **4**.

	<b>x/a</b>	<b>y/b</b>	<b>z/c</b>	<b>U(eq)</b>
H6	0.1180	0.3578	-0.1486	0.033
H7	0.0406	0.2404	-0.1796	0.033
H1	0.4169	0.3003	-0.1813	0.033
H2	0.3294	-0.0995	0.0874	0.027
H8	-0.0332	-0.0947	0.0468	0.027
H3	0.0307	-0.0576	0.1321	0.027
H5	0.9107	0.4499	0.0684	0.016
H4	0.8697	0.2438	0.2054	0.016
H11	1.2793	0.5827	0.6353	0.03
H9	1.2682	0.5924	0.5512	0.03
H16	1.5630	0.5405	0.5860	0.03
H12	0.2571	0.1348	0.3074	0.03
H13	0.2990	0.2524	0.3033	0.03
H10	-0.0233	0.2006	0.3393	0.03
H15	0.2985	0.0584	0.5578	0.016
H14	0.9599	0.2566	0.7006	0.016

**Table S3.7.** Hydrogen bond distances (Å) and angles (°) for **4**.

	<b>Donor-H</b>	<b>Acceptor-H</b>	<b>Donor-Acceptor</b>	<b>Angle</b>
C16-H15...O8	0.95	2.39	3.2985(18)	161.1
C15-H12...Br2	0.98	3.02	3.9415(18)	158.0
C10-H9...N2	0.98	2.61	3.571(2)	166.6
C10-H9...O5	0.98	2.59	3.310(2)	130.0
C7-H5...O4	0.95	2.35	3.2187(17)	151.0
C6-H8...N1	0.98	2.68	3.6416(19)	167.0
C6-H8...O2	0.98	2.61	3.351(2)	132.4
C16-H15...O8	0.95	2.39	3.2985(18)	161.1
C15-H12...Br2	0.98	3.02	3.9415(18)	158.0
C10-H9...N2	0.98	2.61	3.571(2)	166.6
C10-H9...O5	0.98	2.59	3.310(2)	130.0
C7-H5...O4	0.95	2.35	3.2187(17)	151.0
C6-H8...N1	0.98	2.68	3.6416(19)	167.0
C6-H8...O2	0.98	2.61	3.351(2)	132.4
C6-H8...O2	0.98	2.61	3.351(2)	132.4
C6-H8...N1	0.98	2.68	3.6416(19)	167.0
C7-H5...O4	0.95	2.35	3.2187(17)	151.0
C10-H9...O5	0.98	2.59	3.310(2)	130.0
C10-H9...N2	0.98	2.61	3.571(2)	166.6
C15-H12...Br2	0.98	3.02	3.9415(18)	158.0
C16-H15...O8	0.95	2.39	3.2985(18)	161.1

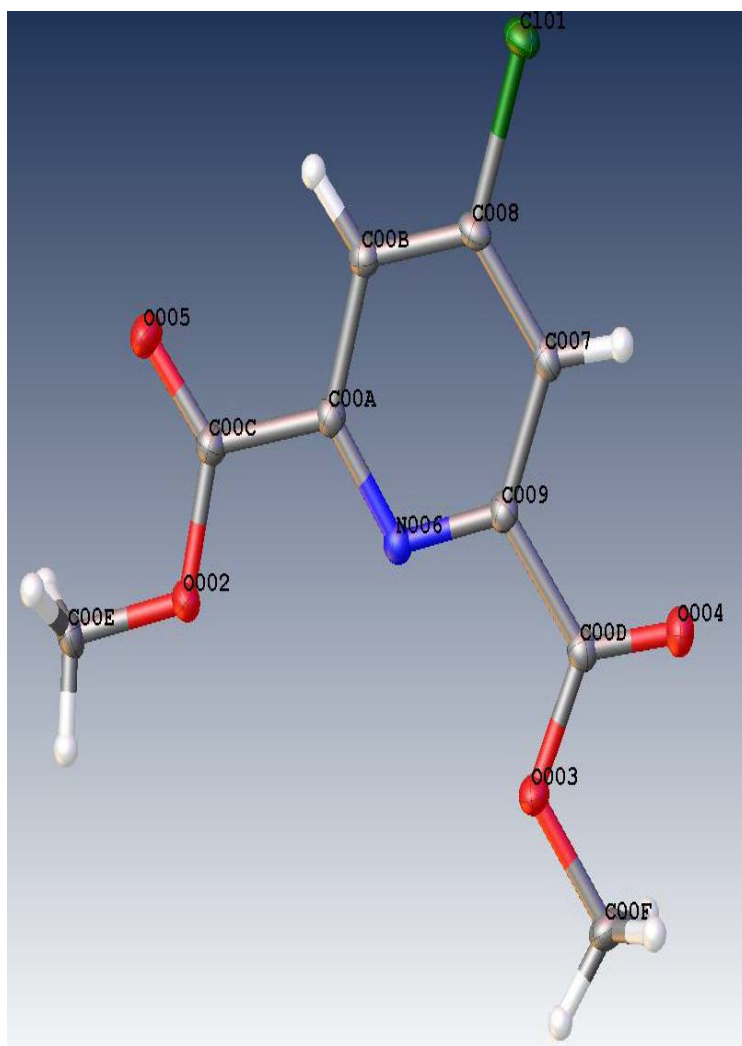


**Figure S3.** Thermal ellipsoid (50%) plot of **5** with labeling schemes adopted.

**Table S4.1.** Fractional Atomic Coordinates ( $\times 10^4$ ) and Equivalent Isotropic Displacement Parameters ( $\text{\AA}^2 \times 10^3$ ) for **5**.

Atom	x	y	z	U(eq)
Cl01	1415.06(3)	3765.12(3)	1318.90(3)	19.36(7)
O002	7551.03(3)	5405.10(3)	4317.51(3)	18.61(14)
O003	9002.94(3)	2104.88(3)	4169.57(3)	19.07(14)
O004	6634.00(3)	1208.40(3)	3256.18(3)	21.81(15)
O005	4490.04(3)	6265.56(3)	3473.49(3)	25.41(16)
N006	6503.62(3)	3749.29(3)	3583.87(3)	13.48(15)
C007	4492.72(3)	2888.88(3)	2493.69(3)	14.76(17)
C008	3319.69(3)	3756.30(3)	2191.77(3)	14.27(16)
C009	6050.03(3)	2933.85(3)	3193.64(3)	13.27(16)
C00A	5299.68(3)	4568.81(3)	3274.18(3)	13.59(16)
C00B	3672.90(3)	4619.25(3)	2579.78(3)	14.77(17)
C00C	5711.24(3)	5508.36(3)	3693.79(3)	15.73(17)
C00D	7244.80(3)	1988.50(3)	3531.38(3)	14.64(17)
C00E	8044.09(3)	6293.44(3)	4741.01(3)	19.67(18)
C00F	10132.08(3)	1207.87(3)	4514.44(3)	20.19(18)

**Table S4.2.** Bond Lengths ( $\text{\AA}$ ) for **5**.

Cl01	C008	1.7369(5)	N006	C00A	1.3393(3)
O002	C00C	1.3328(3)	C007	C008	1.3860(3)
O002	C00E	1.4567(3)	C007	C009	1.3987(4)
O003	C00D	1.3417(3)	C008	C00B	1.3881(3)
O003	C00F	1.4480(3)	C009	C00D	1.5071(4)
O004	C00D	1.2064(3)	C00A	C00B	1.4011(4)
O005	C00C	1.2079(3)	C00A	C00C	1.5096(4)
N006	C009	1.3387(3)			

**Table S4.3.** Bond Angles ( $^\circ$ ) for **5**.

C00E	O002	C00C	115.034(4)	C00B	C00A	N006	124.429(4)
C00F	O003	C00D	114.493(4)	C00C	C00A	N006	118.488(4)
C00A	N006	C009	116.287(5)	C00C	C00A	C00B	117.083(4)
C009	C007	C008	116.919(4)	C00A	C00B	C008	117.060(4)
C007	C008	Cl01	119.763(4)	O005	C00C	O002	124.737(5)
C00B	C008	Cl01	119.712(4)	C00A	C00C	O002	112.883(4)
C00B	C008	C007	120.524(5)	C00A	C00C	O005	122.379(5)
C007	C009	N006	124.766(4)	O004	C00D	O003	123.813(4)
C00D	C009	N006	118.188(4)	C009	C00D	O003	113.186(4)
C00D	C009	C007	117.040(4)	C009	C00D	O004	122.996(5)

**Table S4.4.** Anisotropic Displacement Parameters ( $\text{\AA}^2 \times 10^3$ ) for **5**.

Atom	U11	U22	U33	U12	U13	U23
Cl01	23.99(4)	22.13(15)	11.78(13)	-2.24(9)	-4.50(9)	0.99(10)
O002	24.78(4)	14.2(3)	16.5(4)	0.74(14)	-7.10(18)	-1.9(3)
O003	26.51(4)	14.7(3)	15.8(4)	2.58(14)	-5.44(18)	0.1(3)
O004	29.40(4)	14.1(3)	21.8(4)	-0.39(15)	-5.20(18)	-1.5(3)
O005	37.42(4)	16.5(3)	21.9(4)	7.96(15)	-10.22(19)	-2.4(3)
N006	13.14(4)	14.1(3)	13.2(4)	-0.51(14)	0.04(18)	0.1(3)
C007	16.29(4)	15.0(4)	13.0(4)	-2.42(15)	0.34(19)	-0.9(3)
C008	13.92(4)	19.3(4)	9.6(4)	-2.30(15)	-0.52(18)	1.1(3)
C009	13.57(4)	13.7(4)	12.5(4)	-0.51(15)	0.96(18)	0.8(3)
C00A	13.73(4)	14.3(4)	12.8(4)	-0.39(15)	0.50(18)	0.2(3)
C00B	15.14(4)	15.6(4)	13.5(4)	-0.11(15)	-0.38(19)	1.6(4)
C00C	17.29(4)	16.0(4)	13.8(4)	0.38(15)	-1.05(19)	-0.1(4)
C00D	15.05(4)	15.6(4)	13.4(4)	0.08(15)	1.33(19)	0.2(4)
C00E	23.84(4)	16.3(4)	18.7(5)	-0.28(15)	-5.22(19)	-5.3(4)
C00F	22.82(4)	19.3(4)	18.4(5)	5.36(15)	-1.58(19)	4.2(4)

**Table S4.5.** Hydrogen Atom Coordinates ( $\text{\AA} \times 10^4$ ) and Isotropic Displacement Parameters ( $\text{\AA}^2 \times 10^3$ ) for **5**.

Atom	x	y	z	U(eq)
H00B	2882.11(3)	5226.68(3)	2384.10(3)	23.944(3)
H00a	9200.75(3)	6776.42(3)	4437.88(3)	22.535(3)
H007	4264.55(3)	2304.81(3)	2252.26(3)	26.788(3)
H00e	11572.72(3)	891.05(3)	4194.09(3)	23.175(3)
H00f	8009.97(3)	855.55(3)	4644.34(3)	26.559(3)
H00g	11555.67(3)	1449.07(3)	4925.03(3)	36.339(3)
H00c	9537.57(3)	6125.04(3)	5134.76(3)	26.109(3)
H00d	5723.39(3)	6552.10(3)	4887.49(3)	22.555(3)

The figure set of thermal ellipsoid (50%) plots with the labeling schemes adopted aid in the clarification of the data tables shown herein. In **Figure S2**, the bond lengths between C8 and Br1 and C17 and Br2 are 1.8818  $\text{\AA}$  and 1.8822  $\text{\AA}$  as shown in **Table S3.2**. Whereas, as seen in **Figure S3**, the bond length between C008 and Cl1 is 1.7369  $\text{\AA}$ , as found in **Table S4.2**. Therefore, the difference between the

average of the Br-C bonds in compound **4** (1.8820 Å) and the Cl-C bond in compound **5** (1.7369 Å) is 0.1451 Å. This occurs as an expected result of the difference in electronegativity between Cl and Br. Considering the fact that Cl is more electronegative than Br, Cl attracts more of the electron density from its bonded carbon than the bonded carbon of the Br, causing the bond length of the Cl-C bond to be shorter than the Br-C bond.

In order to get a more complete picture of this portion of the structures, the bond angles are then evaluated and compared. In compound **4**, according to **Table S3.3**, the angle made by C7-C8-Br1 is 121.02° and the angle made by C18-C17-Br2 is 119.51°. On the other side of the bond, the angle made by C9-C8-Br1 is 120.50° and the angle made by C16-C17-Br2 is 119.47°. Comparatively, in compound **5**, according to **Table S4.3**, the angle made by C00B-C008-Cl01 is 119.712° and the angle made by C007-C008-Cl01 is 119.763°. It is notable that the bond angles in compound **5** are slightly smaller than the bond angles in **4** in this portion of the molecule.

Looking at the carbonyl groups on both compound **4** and **5** aid in the elucidation of the effects of the functionalization of the pyridol core by comparing the bond lengths and angles associated with the C=O bonds in these compounds. As found in **Figure S2**, the relevant bond lengths for the C=O bonds in compound **4** are C2-O4, C5-O3, C11-O7, and C14-O8. These bond lengths are 1.2044 Å, 1.2088 Å, 1.2113 Å, and 1.2071 Å respectively, according to **Table S3.2**. Compared to the relevant bond lengths for compound **5**, as illustrated in **Figure S3**, are C00C-O005 and C00D-O004. These bond lengths are 1.2079 Å and 1.2064 Å respectively

according to **Table S4.2**. These bond lengths show no difference between the two compounds that is statistically significant.

The associated bond angles with the carbonyl groups of **4**, in accordance with **Figure S2**, are O1-C2-O4, C3-C2-O4, O2-C5-O3, C4-C5-O3, O5-C11-O7, C12-C11-O7, O6-C14-O8, and C13-C14-O8. These bond angles are 123.74°, 123.20°, 125.33°, 121.71°, 125.04°, 122.17°, 124.36°, and 122.80°, respectively, in accordance with **Table S3.3**. While these bond angles do have a relatively sizable range of 3.62°, they all center evenly around their mean, 123.54°. The comparable bond angles for compound **5**, shown in **Figure S3**, are O002-C00C-O005, C00A-C00C-O005, O003-C00D-O004, and C009-C00D-O004. This data, from **Table S4.3**, reveals these bond angles to be 124.737°, 122.379°, 123.813°, and 122.996°, respectively. Notably, there is less variability in these numbers when compared to those of compound **4**, considering the range of these is 2.358°. The mean of these values is 123.48°, which is similar to the results found for compound **4**. These results indicate that the functionalization of the pyridol core with either Br or Cl will not have an impact on the angles associated with the carbonyl group.

**REFERENCES**

1. Alzheimer's Disease Facts and Figures, Alzheimer's & Dementia. Alzheimer's Association 2011, 7.
2. (a) Lincoln, K. M.; Gonzalez, P.; Richardson, T. E.; Julovich, D. A.; Saunders, R.; Simpkins, J. W.; Green, K. N., 'A potent antioxidant small molecule aimed at targeting metal-based oxidative stress in neurodegenerative disorders. *Chem. Commun* 2013, 49, 2712-2714; (b) Lincoln, K. M.; Green, K. N.; Gonzalez, P., Bimodal antioxidant chelators in response to metal-induced aggregation in Alzheimer's disease. Abstracts of Papers, 243rd ACS National Meeting & Exposition, San Diego, CA, United States, March 25-March 29, 2012 2012, BIOL-229; (c) Lincoln, K. M.; Offutt, M. E.; Hayden, T. D.; Saunders, R. E.; Green, K. N., Structural, Spectral, and Electrochemical Properties of Nickel(II), Copper(II), and Zinc(II) Complexes Containing 12-Membered Pyridine- and Pyridol-Based Tetra-aza Macrocycles. *Inorg Chem* 2014, 53 (3), 1406- 1416.
3. Jagannath B. Lamture, Z. Hong Zhou, A. Suresh Kumar, and Theodore G. Wensel., Luminescence Properties of Terbium(III) Complexes with 4-Substituted Dipicolinic Acid Analogues. *Inorg. Chem.* 1995, 34, 864-869.